Bi-monthly • July - August • 2018
ISSN: 0976-2108

BARC NEWSLETTER

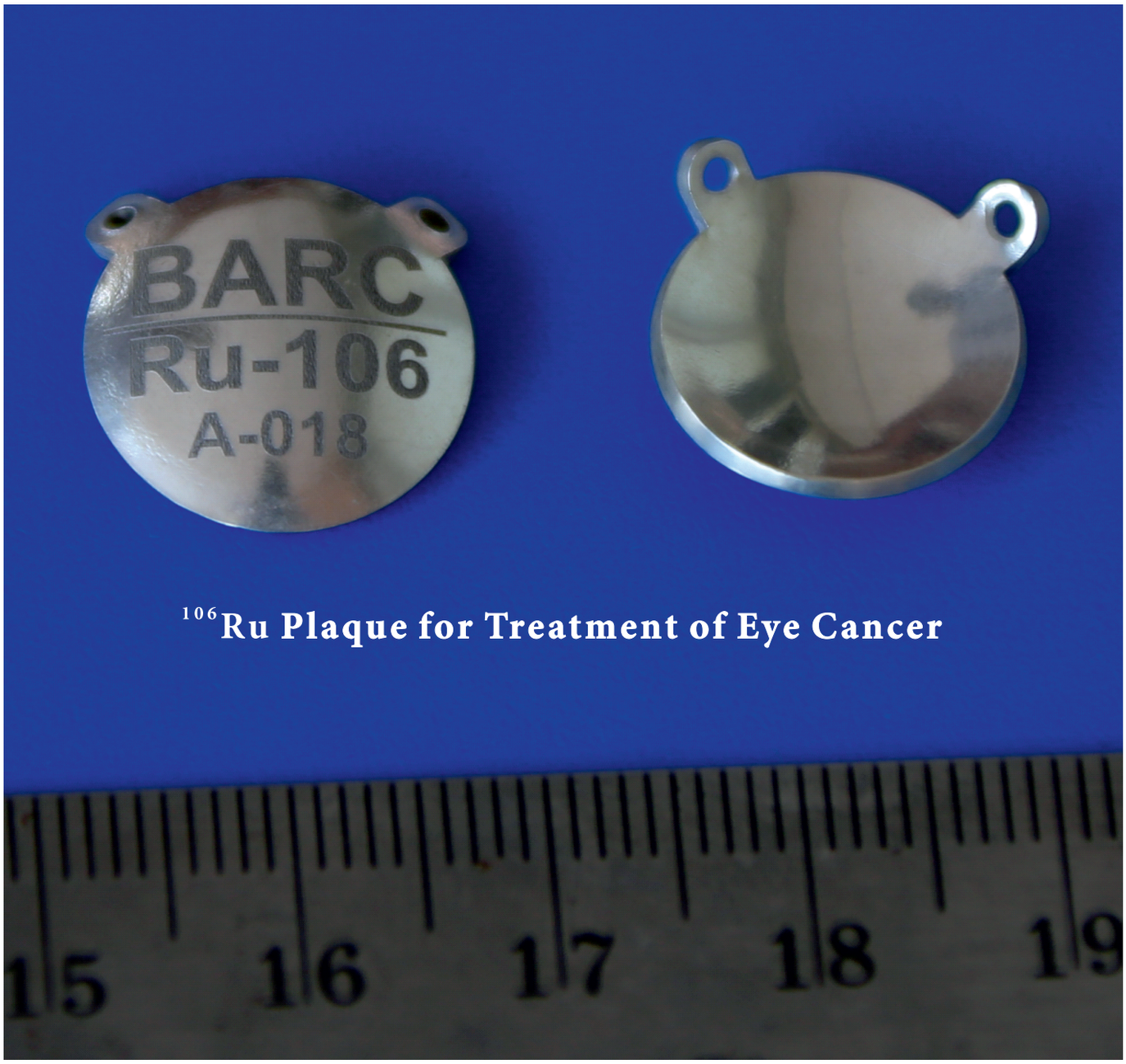

^{106}Ru Plaque for Treatment of Eye Cancer

CONTENTS

Development of ^{106}Ru bearing Sealed Source for Eye Cancer Treatment Applications

Prithwish Sinharoy, Dayamoy Banerjee, Rohit Gupta, Arvind Ananthanarayanan, Ramakant, Pawan D. Maniyar, Jayesh G. Shah, Kailash Agarwal, Smitha Manohar and Chetan Prakash Kaushik
Nuclear Recycle Group, Bhabha Atomic Research Centre, Trombay, Mumbai

Abstract

Use of ^{106}Ru plaque in brachytherapy is a proven technique for treatment of different eye cancers. However, ubiquitous availability of this treatment modality is limited due to highly expensive imported sources. The present communication showcases indigenous development of ^{106}Ru based plaque source, starting from separation of the fissiogenic radionuclide from High Level Waste (HLW) followed by its immobilization onto silver substrate and finally its encapsulation into silver plaque. Evidently, availability of indigenous sources will greatly help in reducing the cost of brachytherapy and help save vision.

Keywords : ^{106}Ru plaque, eye cancer, ocular tumor, radioactive waste, electrodeposition, sealed source.

Introduction

Choroidal melanoma and retinoblastoma are the most commonly occurring cancers of the eye in adults and in children, respectively [1–3]. As the first solution, ophthalmic oncologists prefer plaque radiotherapy owing to the simplicity and flexibility associated with the technique [1, 3]. Indeed, depending upon the location and extent of the melanoma, plaques with different geometries and varying strength are being used for irradiation [1]. Various radionuclides such as ^{60}Co, ^{106}Ru, ^{125}I, ^{103}Pd, ^{90}Sr, and ^{131}Cs were used in making ophthalmic plaques. However, most commonly used ophthalmic plaques are ^{125}I and ^{106}Ru [1, 4]. ^{106}Ru decays by emission of high energy β-rays, while ^{125}I decays by electron capture to an excited state of Tellurium-125 and thereby emits low energy gamma radiation. Indigenous development of ^{125}I plaque has been discussed elsewhere [5]. Present efforts were directed to develop ^{106}Ru plaque indigenously.

The use of ^{106}Ru based plaque is more convenient to doctors. This may possibly due to relatively longer half life of ^{106}Ru. Further, β-radiation has a limited range, leading to a steep dose fall-off, allowing tumours (upto 5mm) to be treated while minimizing inadvertent irradiation of sensitive ocular structures such as the fovea or the optic disc [1 – 4].

Unlike ^{125}I, which can easily be synthesized in chemically pure form, ^{106}Ru is available only in the nuclear waste generated from reprocessing of spent fuel. Therefore, isolation of the fission product in chemically pure form is a herculean task. This may be one of the reasons that no Ru plaque has been prepared after separation of the fission products from High Level Waste (HLW). In India, the management of HLW is being carried out by partitioning of long-lived minor actinides and valuable fission products such as ^{137}Cs and ^{90}Sr. The activity lean solution is a treasure trove of ^{106}Ru. Processing a cubic meter of the solution will be adequate for the preparation of thousands of ophthalmic plaques.

In view of the abundant availability of the radioisotope and its potential use in eye cancer treatment, concerted efforts were made, culminating in the fabrication of ^{106}Ru plaque suitable for brachytherapy applications. In this paper, salient features of process development, including flow sheet finalization for recovery of radio-chemically pure ^{106}Ru, fixation of the recovered ^{106}Ru on silver substrate by electro-deposition and fabrication of sealed source have been highlighted.

Experimental

The actual HLW of research reactor origin was initially subjected to separation of ^{137}Cs by Calix crown, followed by co-extraction of minor actinide and Sr by TEHDGA. The resulting activity lean solution is used as the feed in the reported study. Purification of ^{106}Ru in radio chemically pure form was carried out as per the flow diagram given in **Fig.1**. In the first step, KIO_4 (s) was added to convert Ru species to RuO_4, which was then extracted using CCl_4 pre-equilibrated with Cl_2. The extracted ruthenium was stripped back using 0.1 M hydrazine in 1 M nitric acid. The strip solution was dried and the residue after dissolving in 4 % sulphamic acid was used as catholyte. The ^{106}Ru was electrochemically deposited on Ag cathode using Pt anode and sulphamic acid as anolyte. The Ru deposited cathode was further used for plaque preparation.

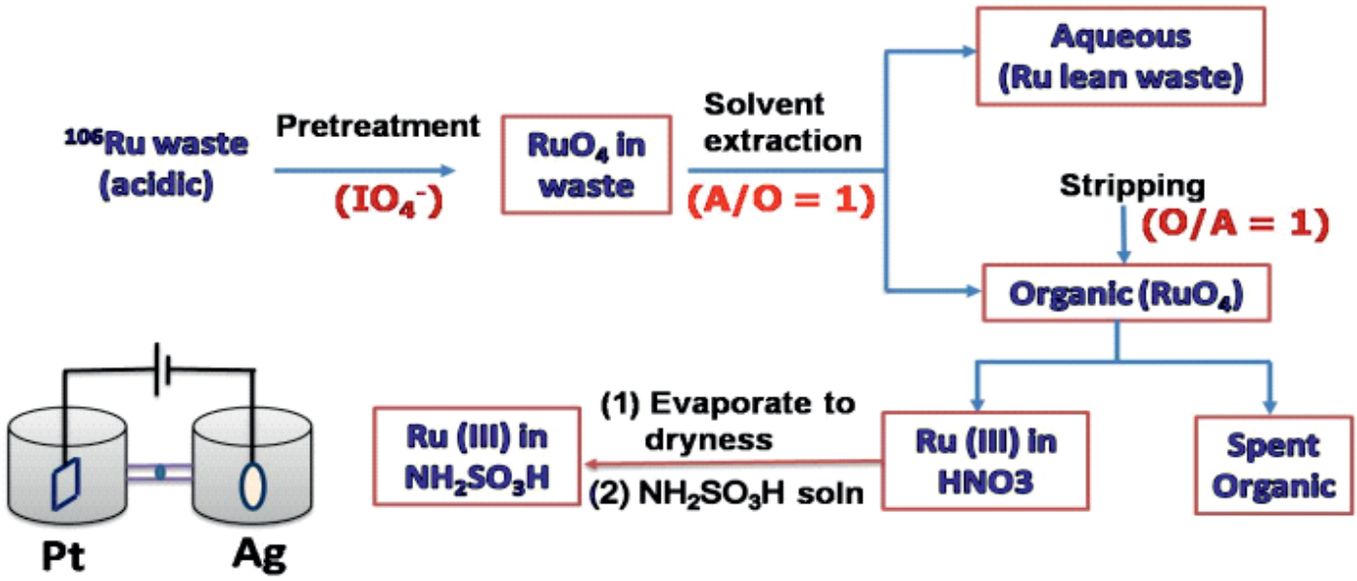

Fig. 1: Schematic flow sheet depicting ^{106}Ru extraction from HLW and subsequent electrodeposition on Ag

The plaque consists of a 0.9 mm thick Ag backing plate (dia 15.8 mm), the 0.2 mm thick Ru coated Ag substrate and a 0.1mm thick Ag window (dia 16 mm). The entire assembly was sealed using an Ag based brazing alloy. For the sealing operation, the plaque was assembled on a graphite jig, which was then placed in an all quartz bell jar assembly maintaining an Ar atmosphere. This assembly was introduced into the furnace preheated at 870°C in a controlled manner and withdrawn after about 2 minutes, for cooling under ambient condition. Post cooling, the plaque was bent to the required radius using a die.

Results and Discussions

The waste feed used in this study was relatively clean and contains only traces of ^{137}Cs (0.1 mCi/l) and almost equal amount of ^{106}Ru and ^{125}Sb (30 mCi/l). For the selective separation, Ru species were oxidized to RuO_4 and extracted in CCl_4. The extent of extraction was studied by varying aqueous to organic (A:O) ratio. It was found that almost 80% of ^{106}Ru can be extracted using A:O ratio of 1 in a single contact. The decrease of organic volume reduced the extent of extraction, but not significantly. Almost 73% of ruthenium was extracted to the organic phase in a single contact using A:O ratio of 3. It was observed that extraction of RuO_4 in CCl_4 is quite rapid and complete equilibration was attained within 10 minutes. This is possibly due to very high solubility of the RuO_4 in CCl_4. As RuO_4 is highly volatile, extraction was carried out under closed conditions to minimize the volatilization loss of the radioelement. Further, RuO_4 is highly unstable and can be reduced easily to RuO_2 upon contact with any organic medium. An oxidative condition is therefore mandatory to maintain RuO_4 in CCl_4. This was achieved using Cl_2 gas equilibrated CCl_4. Stripping of the RuO_4 from CCl_4 phase was carried out after reducing the RuO_4 to Ru(III).

Considering the source preparation by electro-deposition method, a medium directly suitable for electrolysis such as sulphamic acid, was considered to be the ideal choice. The use of sulphamic acid, alone and with hydrazine was attempted. Due to poor stripping efficiency of the previously mentioned processes, hydrazine in HNO_3 was used. Under these conditions also, a long equilibration time of at least 1 hour was required to achieve quantitative stripping. The stripped solution was analyzed using HPGE detector coupled with 8K MCA. No peaks other than gamma peaks for ^{106}Ru are seen, indicating that the process is effective in separating Ru in radiochemically pure form. By adjusting, aqueous organic ratio, both in extraction and stripping steps, it is possible to get a concentrated solution of ^{106}Ru.

Prior to electrodeposition of ^{106}Ru, the strip solution was evaporated to mitigate nitrate interference during deposition. The residue was dissolved in 4% (wt.) sulphamic acid and used as catholyte. It is to be noted that the Ru concentration in the catholyte is quite low (< 300 ppm) and about 300 μCi of ^{106}Ru needs to be deposited on a substrate of diameter 12.7 mm. To achieve this, while obtaining a uniform and adherent coating, several inactive coating trials were carried using simulated waste. The coated samples were analyzed using SEM and EDS, with the results being presented in **Fig. 2**.

An inspection of **Fig. 2** indicates that in case of high current density of 65 $mA.cm^{-2}$ (left), the coating is thick and layered. This coating is not uniform and quite rough. Further, the colour of the coating in case of high current density is black indicating some oxidation of the deposited Ru.

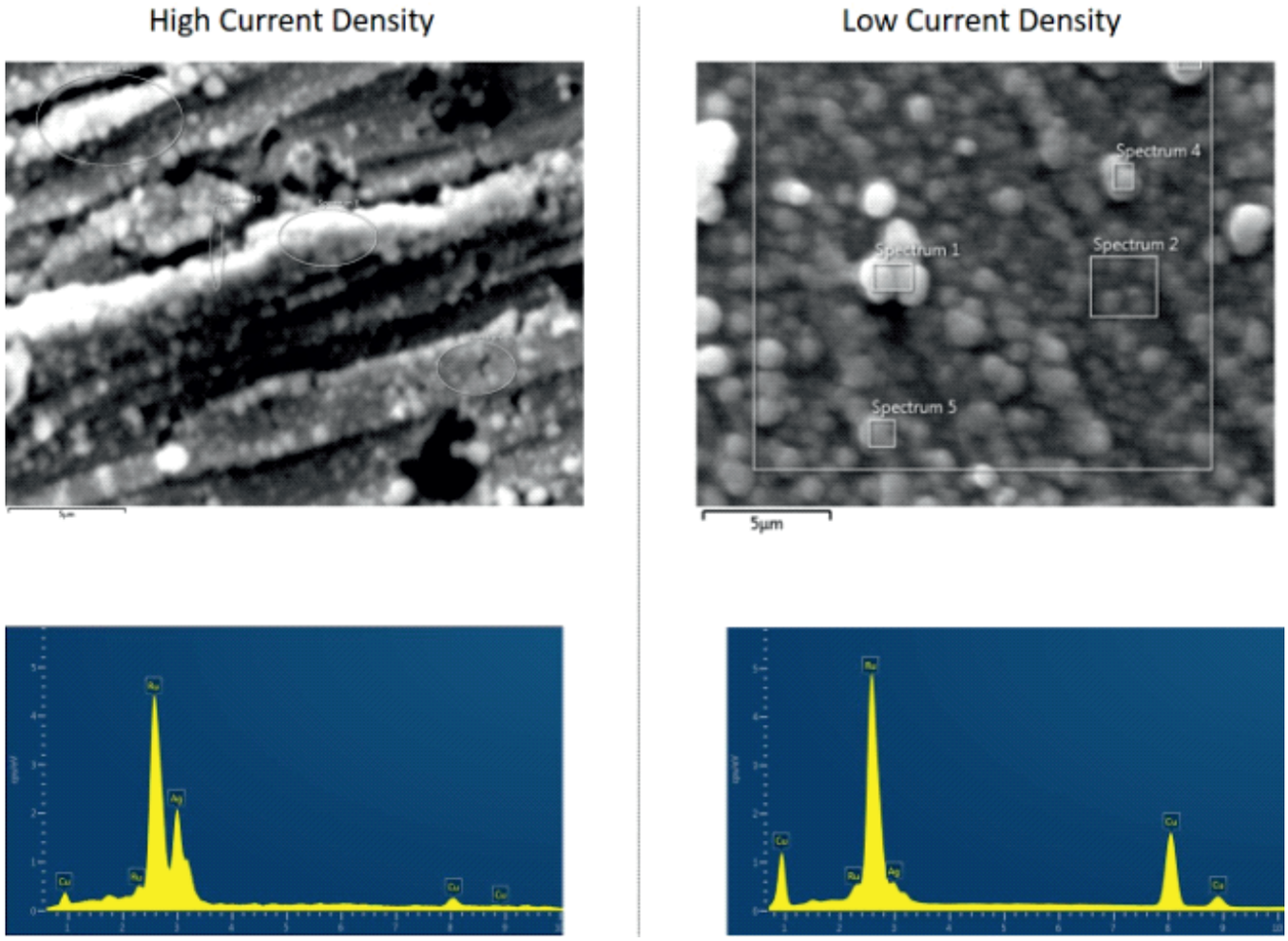

Fig. 2: SEM micrograph of ^{106}Ru deposited electrolytically on Ag at different current densities. The lower images are the EDS spectra of these samples

In comparison, at low current density of 5 mA.cm^{-2}, (right), a more uniform coating of Ru metal on the substrate is obtained. Oxidation is also lesser than the high current density case, as evident from the silvery grey colour of the coating. The optimized current density of 5 mA.cm^{-2} was selected and coating studies were carried out with active Ru containing solutions for various periods up to ~ 80 h. The optimized electrodeposition conditions are in good agreement with the earlier study [6]. In all cases, the coated source was washed thoroughly in boiling water before dispatch for activity measurement. **Table 2** collects the activity and dose rate profile of the sources.

The final stage is the fabrication of the ^{106}Ru sealed source. Briefly, the sealed source comprises the 0.2 mm thick source piece in a sandwiched geometry between a 0.9 mm thick backing plate and a 0.1 mm thick window. As mentioned previously, sealing was carried out under Ar atmosphere. This served the twin objectives of minimization of Ru volatilization and preservation of the graphite jig.

After preparation of more than 20 inactive plaques, first active source sealing was carried out using a 25 µCi source. During the sealing air activity was constantly monitored to check for Ru escape. Almost negligible Ru counts were recorded on the sample. Finally, the sealed plaque was bent to the required radius on a die. A file photograph of a Ru plaque is presented in **Fig. 3**.

Table 2: Activity and dose profiles of various ^{106}Ru plaque sources

Sample no	^{106}Ru activity (µCi)	Dose rate at 1 cm (mR/h)
Ru-1	80	100
Ru-2	50	50
Ru-3	25	40
Ru-4	210	400
Ru-5	282	600
Ru-6	367	600

The active Ru plaque was tested for surface contamination by swipe samples and sealing integrity was ascertained by boiling water test for 3 cycles of 20 minutes each. Counting revealed no activity in the immersion liquid. All inactive plaques qualified type classification tests carried out as per AERB SS3 procedure. The plaque design has got approval from AERB for clinical trials at hospitals.

Conclusion

The present study demonstrates isolation of radiochemically pure ^{106}Ru from HLW. An electrodeposition

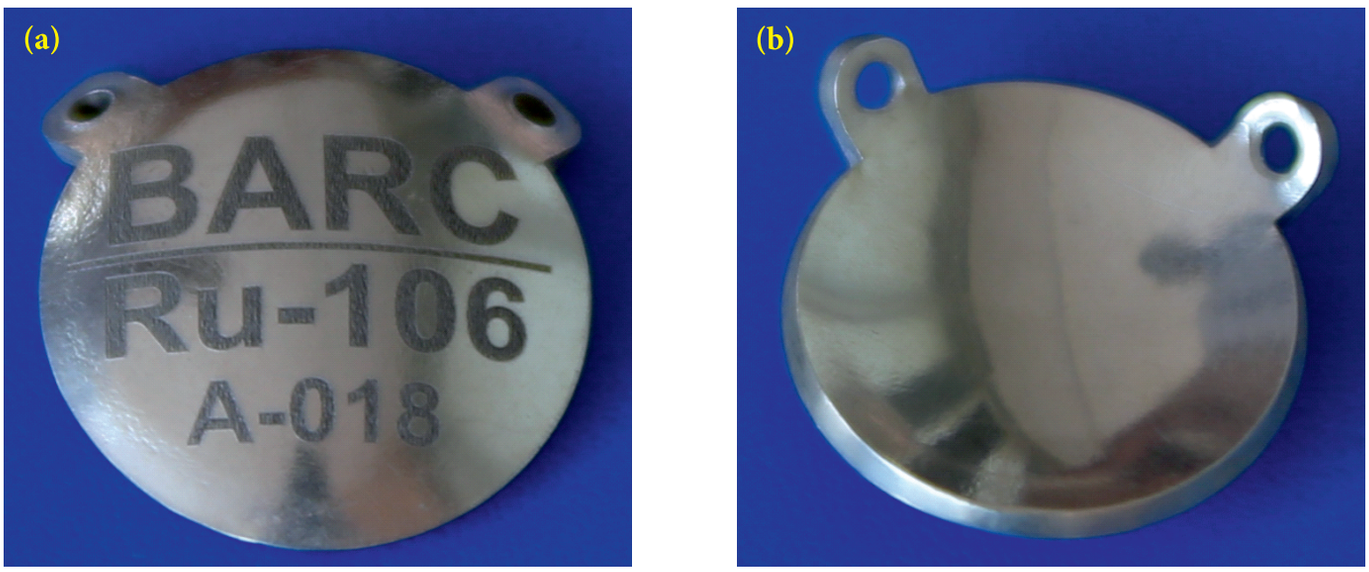

Fig. 3: File photograph of ^{106}Ru plaque (a) Top view and (b) Rear view

process for immobilization of metallic ^{106}Ru on Ag substrate has been optimized and used for source preparation. An innovative sealing process led to the realization of ^{106}Ru brachytherapy plaque. Indeed, this is the third radionuclide, after ^{137}Cs and ^{90}Sr, to be isolated from HLW for societal benefit.

Corresponding author and email: Dr. Dayamoy Banerjee (daya@barc.gov.in)

Acknowledgements

The authors wholeheartedly thank Messer Ajay Manjrekar, Sunil Babu Shinde, S. Langhi, V. M. Phalke, V. K. Kulkarni and Anil Kumar for their involvement in various stages of this work. Sincere thanks to Drs. R. K. Mishra, Amar Kumar and Darshit Mehta for providing Cs lean waste solution used in this study.

References

1. B. H. A. Lee, J. W. Kim, H. Deng, N. Rayees, R. L. Jennelle, S. Y. Zhou, M. A. Astrahan and J. L. Berry, Outcomes of choroidal melanomas treated with eye physics plaques: A 25-year review, Brachytherapy, **2018**, 17(6), 981 – 989.
2. B. Damato, Ocular treatment of choroidal melanoma in relation to the prevention of metastatic death - A personal view, Prog. Ret. Eye Research, **2018**, 66, 187 – 199.
3. H. Mishra, R. Mishra and R. Hadi, A review on retinoblastoma: Most common intraocular malignancy in childhood, Int. J. Sci. Res., **2017**, 6(9), 197 – 199.
4. H. Abouzeid, R. Moeckli, M-C. Gaillard, M. Beck-Popovic, A. Pica, L. Zografos, A. Balmer, S, Pampallona and F. L. Munier, ^{106}Ruthenium Brachytherapy for Retinoblastoma, Int. J. Rad. Oncl. Bio. Phys., **2008**, 71(3), 821 – 828.
5. S. K. Saxena, C. Mathew, S. A. Balakrishnan, M. A. Majali, R. B. Manolkar, S. U. Sane, R. Ram, M. R. A. Pillai, Development of Miniature "BARC $^{[125]}$ Ocu-Prosta Seeds" for the Treatment of Eye and Prostrate Cancers, BARC Newsletter, **2004**, 243, 1 – 11.
6. R.B. Manolkar, A.R. Mathakar and A. Dash, K.P. Muthe, P. Sreeramakrishnan, C.P. Kaushik, Studies on the preparation of ^{106}Ru silver plaque sources for the treatment of eye cancer BARC Newsletter, Issue No. 309 , October **2009** , 39.

Automated Spacer Wire Wrapping System for PFBR Fuel Elements

P. S. Somayajulu, Rajashree Dixit, Prateek Pareek, Farman Ali
Madhusudan Sharma and Anupam Saraswat
Radiometallurgy Division,
Bhabha Atomic Research Centre, Mumbai

Abstract

Fuel for the future cores of Prototype Fast Breeder Reactor (PFBR) will involve plutonium reprocessed from short-cooled high burn-up spent fuel. Fabrication of this fuel presently involves various activities resulting in high man-rem consumption by the operator owing to its high specific activity. The challenges are further compounded due to requirement of high production rate. Automation of the fabrication processes is a necessity to counteract this challenge. Spacer wire wrapping of the fuel pins is one of the process steps which involves high exposure to operator. A fully automated and remotized system was conceptualized, designed and developed for spacer wire wrapping of the fuel elements as a part of achieving this objective. The key design feature of the system was to fully automate the operation cycle and also its integration, in order to completely eliminate manual intervention while achieving the stringent quality specifications of the fuel element.

Keywords: PFBR, Fuel pin, Spacer wire wrapping, Pitch, Crimping, Spot Welding, Automation.

Introduction

Presently, MOX fuel elements for PFBR are fabricated at Fuel Fabrication (FF) Facility at Tarapur wherein pin fabrication operations require frequent operator intervention. PFBR fuel pin fabrication to meet the reload requirements is associated with very high radiological hazard due to high content of plutonium sourced from short cooled recycled fuel leading to operator exposure during manual interventions. Therefore, complete automation of the process has been an important objective during setting up of Fuel Fabrication Plant (FFP).

Spacer wire wrapping of the fuel pins is an operator intensive process step which requires operator to perform handling of the pins and spacer wires; engaging the bead in bottom end plug slot; engaging of the pin in the machine; cutting of spacer wire, disengagement of the wrapped pin from machine and its transfer to spot welding station. A fully automated wire wrapping system was conceptualised to minimise man-rem and ensure damage-free handling of the pin in a high throughput fabrication facility. The system was developed by integrating the wire wrapping and spot welding operations. The machine carried out every cycle of operation in a pin specific manner by measuring the length and end plug offset angle in advance and then controlling the operation appropriately to achieve the correct pitch of wire wrapping on each pin. It has distinct features to ensure safe and efficient sequential operations on eight pins placed on a tray, without any manual intervention.

Fuel for the upcoming Prototype Fast Breeder Reactor (PFBR) is Uranium-Plutonium mixed oxide (MOX). The fuel pellets are annular in shape and stacked in D9 clad along with axial blankets on either sides. The loaded fuel pins are hermetically sealed by welding end plugs at both ends. The welded fuel pins are wrapped with D9 spacer wires with a specified pitch of wrapping. The spacer wire has a bead at one end to be entangled to the groove provided on the bottom end plug of the fuel pin. The top end plug has a slot through which the wire requires to pass precisely, and is crimped. The wire is welded on the top end plug by spot welding [1].

The length and diameter for PFBR fuel pin are 2580 ± 5 mm and 6.6 ± 0.02 mm respectively [2]. The spacer wire diameter and pitch of wrapping are 1.6 ± 0.02 mm and 200 ± 5 mm respectively [2, 3]. The schematic of wire wrapped fuel pin for PFBR is shown in **Fig. 1** [4].

The spacer wire is wrapped to ensure consistent coolant flow resulting in

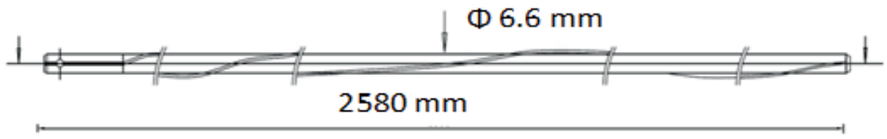

Fig.1: Schematic of PFBR fuel pin

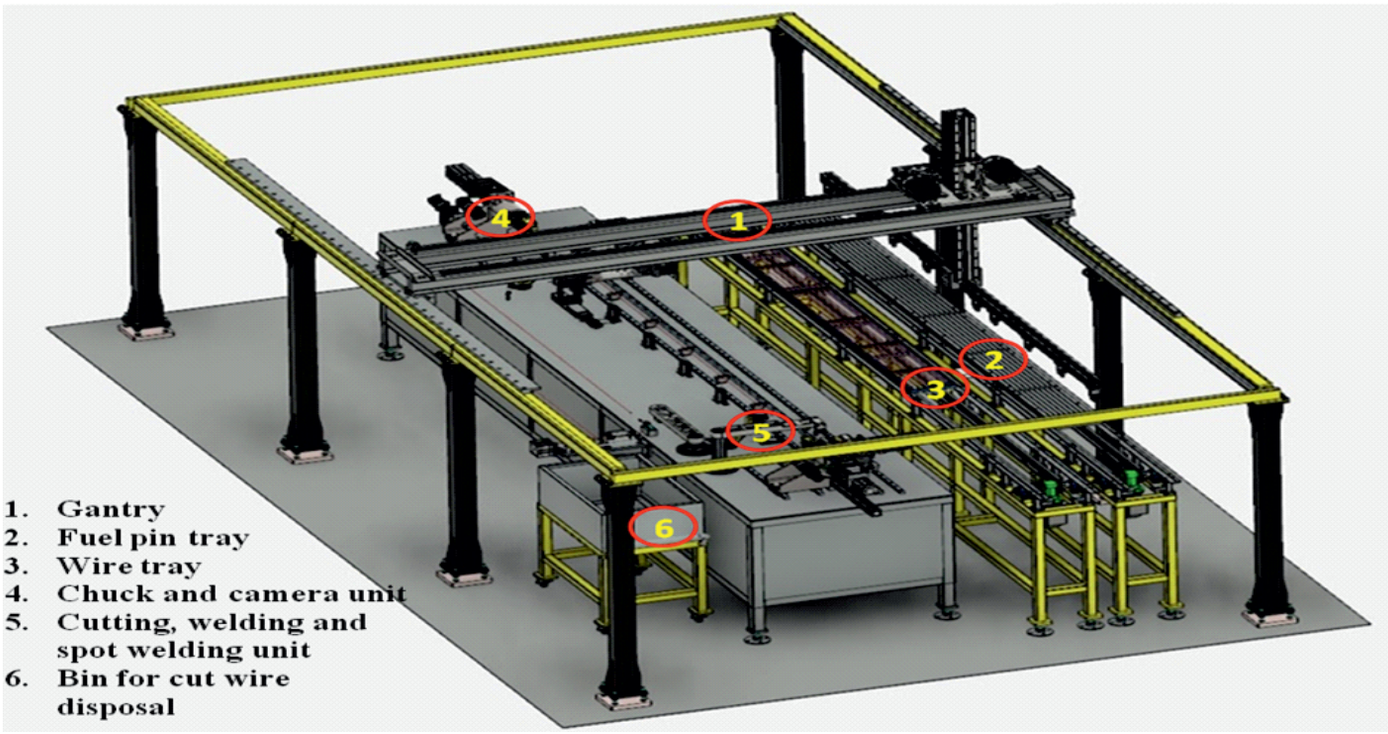

Fig. 2: Schematic diagram of wire wrapping system

efficient heat transfer. The diameter of the spacer wire and pitch of the wrap is specified to ensure stable thermo hydraulics of the coolant in the reactor. It is also crucial to ensure the tightness of wire wrap to maintain consistency in heat transfer. The wire is wound with a tension of 5-7 Kg to ensure no gap between the wire and the pin [1]. Any variation in these characteristics of the pin may lead to distortion in coolant flow pattern and thereby generation of thermo-mechanical stresses on the pin.

Methodology

The automated wire wrapping system is broadly divided into two parts, namely the mechanical part and the control part. The mechanical part consists of gantry system with gripper assembly, tray tables with push and pull mechanism and wire wrapping system consisting of several subsystems for pin handling, wire handling, pin positioning & rotating, wire feeding (engaging of bead and wrapping around the pin), wire crimping, wire cutting & disposal and spot welding. Pin tray and wire tray having 8 pins and 8 wires respectively and are positioned adjacent to work table under the gantry for handling. The control part consists of a motion controller, PC for operation control & monitoring, servo motors and sensor circuitry. The wire wrapping system also has a UPS system with a battery backup of 20 minutes. The system developed is fully automated and undergoes a sequential operation in every cycle. The schematic of the system designed is shown in **Fig 2**.

The sequence of operation which gets repeated for eight times for each tray is as follows. The pin handling system consists of a XY manipulator with specially designed Teflon grippers to ensure scratch proof handling of pins. The two degrees of freedom of the manipulator are servo driven and are precisely controlled. The manipulator has eight equi-spaced grippers to ensure sufficient support to the pin thereby eliminating sagging. The grippers are normally closed to ensure fail-safe operation and are actuated to open. The grippers pick and place the pin from the tray on the V-support provided on the work table. The grippers also pick the wire and place it near the work table where it is engaged with a roller assembly and a jaw. Two chucks with individual motor control are provided on either side of the V-support on which the pin is positioned on the work table.

The length of the pin is first measured with a LVDT before it is held with the chuck near the top-end plug. A camera based sensor is placed near the chuck adjacent to the bottom-end plug which is used to capture its images through indexed rotations of the pin using the chuck rotation. These images are used to check the orientation of the groove on the bottom-end plug for engaging the wire appropriately. Once the pin gets so aligned, the bead of the wire is engaged to the groove with the help of the roller assembly in which it is held. The rollers undertake differential motion in such a way that the wire bends and enters the groove on the bottom end plug.

An additional plate with a V-groove is placed subsequent to the roller assembly such that the wire retraces its path to the groove even if the alignment is not proper on account of the mechanical stiffness. After the roller engages the wire into the grove, the jaw pulls it to provide the desired

tension to the wire to arrest the bead in the groove. The chuck near the bottom-end plug holds the pin for further operation and releases it from the other chuck. Another camera based sensor is placed near the chuck adjacent to the top end plug to check the orientation of the top end plug slot by indexed rotation of the pin.

The angular offset of the top-end plug slot from the bottom end plug groove is calculated using this indexed rotation of the chuck and ensured to be within 270° ± 15°, based on which the pin is either taken up for wire wrapping or rejected. The measured values of pin length and the angular offset of end plugs are used to calculate the speed of rotation of the chuck to ensure a pitch within the specified range (200 ± 5 mm). The jaw holding the spacer wire is moved along the length of the pin in synchronisation with the pin rotation to ensure gapless wrapping of the wire.

Post the wrapping of the wire on pin, the crimping head aligns itself onto the top-end plug and crimps the wire into the slot such that the wire is tightly held in position with desired tension. The wire is spot welded in the slot using TIG welding to ensure stability during irradiation. After the spot welding,

a cutting tool cuts the extra length of the wire and an additional pick-and-place system (gripper) disposes the cut piece of wire to a trash bin. After the operations are completed, the pin handling system picks the wire wrapped pin and places it back in the pin tray in the position from where the unwrapped pin was selected.

The PC based control system enables the operator to start the process of wire-wrapping after a tray is placed in the predefined location. The manipulator performs indexed movement for completing the operation on all the eight pins. The manipulator starts the operation from the first position of the pin on the tray and repeats the sequential operation by indexing its position on the tray till the eight position of the pin tray. However, the operator can intervene to select a pin from any random position of the tray and execute the entire sequence. The system provides a live display of the pitch and tension at which the wire is wound during each operation. The camera based system enables the operator to scrutinize the orientation of the slot, crimping of the wire and pitch of the wrap before proceeding to spot welding.

Fig. 3: Pin and wire handling subsystems.

System Description

The overall dimensions of the system are 7.8 m, 2.9 m and 2 m along X, Y and Z-axes respectively. The fuel pin tray and the wire tray can accommodate eight fuel pins and eight wires, respectively. The spacer wires are pre-cut to a length of 3500 mm. Both the trays are made of stainless steel base for support and aluminium profile with V-groove along with U clips for holding and latching the fuel pins and wires.

The pin and wire handling subsystem is specially designed to pick and place the fuel pins and wires to the location of wire wrapping in the system as shown in **Fig 3**. There are eight equi-spaced rhombus shaped grippers for gripping the pins and wires from the respective trays. These grippers are Teflon coated so as to prevent any damage on the surface of the pin.

The optical sensor used for the top and bottom end plug has a standard resolution of 640x480 pixels with a 2X magnification. It has a 32 MB flash memory and unlimited memory through remote network device. **Fig. 4** shows the actual photograph of the camera placed near the chuck.

The system is mounted over LM Guide and ball screws of 4000 mm length, 20 mm diameter & 5mm pitch and moves through the complete length of the pin while the pin rotates along its axis.

Crimping force is applied using a mandrel hydraulically. The crimping force is ensured to be sufficient enough to engage the wire into the top-end plug slot but does not cause any damage to the pin. After it is

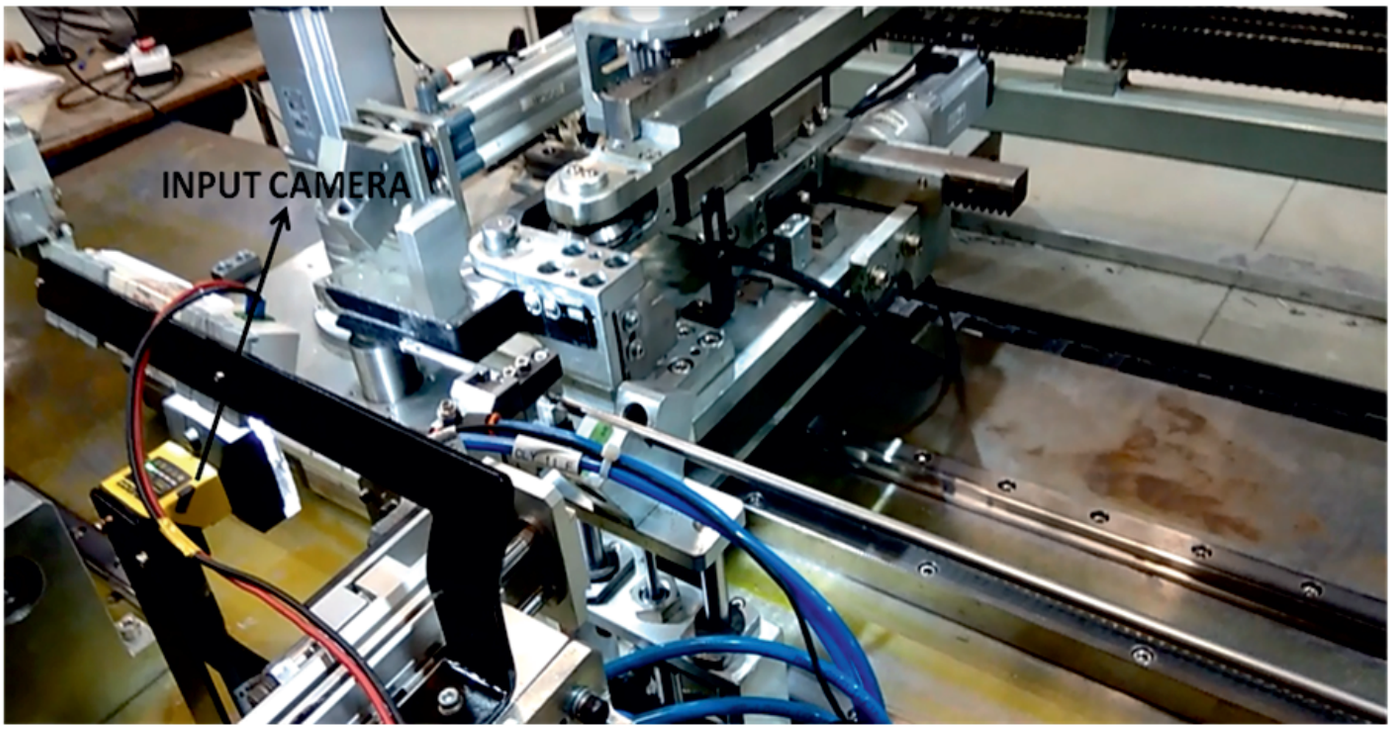

Fig. 4: Input camera placed near the chuck.

crimped, the wire is cut with a scissor-like arrangement and is disposed in a bin. The pick-and-place mechanism lifts the wire-wrapped pin and places it on the welding station adjacent to the wrapping system where the wire is welded onto the pin by spot welding. Proper orientation of the pin for welding and positioning is ascertained using the automated movement of the chuck. The precise positioning of welding electrode is adjusted and monitored remotely using a camera. The spot-weld electrode has a circular cross section and area slightly greater than that of wire so as to provide sufficient weld area. The spot-weld is carried out at 230 VAC (single phase) +/- 10%, 50 Hz supply. The rated power and current of the welding machine are 5.4 Kw and 24 Amp respectively with a voltage of 56 V. **Figure 5(a) and 5(b)** show the camera guided electrode positioning system for welding operation and the welding operation in progress respectively.

The online UPS system operates on 360 VDC, three phase input three phase output supply with an input power factor of 0.9, 50 Hz frequency. Thirty batteries are used to get the desired backup.

Results

Trials were conducted on 20 dummy (without fuel pellets) PFBR fuel pins (D9 SS) with actual PFBR spacer wires. The average operation cycle time was 18 minutes without any manual intervention. The wire wrapped pins were checked for various parameters such as pitch, tension of the wire, visual, dimensional, bow and wire-pin gap and found to be within the specified range of acceptability.

Conclusion

A fully automated spacer wire wrapping and welding system having the following important features has been developed for PFBR fuel pins which significantly contributes to reduction in operator manrem while harmonizing with the high throughput rate and product quality required for PFBR fuel fabrication.

- Salient operational features include:-

» Achieving the specified characteristics on finished fuel pins with good repeatability.

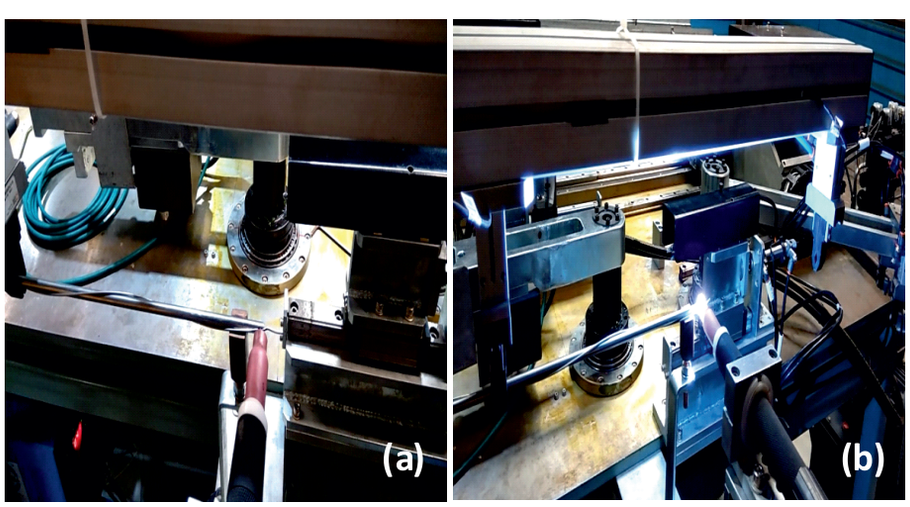

Fig. 5: (a) Camera guided electrode positioning system for welding operation and (b) Welding operation in progress

» Auto-adjustment of operational parameters with respect to the measured length of each fuel element length to ascertain the required pitch.

» Auto conformance check of end plugs orientation (automatic) for acceptance prior to wire wrapping operation.

» Flexibility of carrying out operations on any randomly selected pin in a semi auto operation in addition to the auto sequential operation from a tray loaded with eight pins.

» System designed to ensure appropriate bead engagement in bottom end plug irrespective of wire distortion.

» Remote monitoring, operation and control of the system.

· Operational safety features incorporated for fail safe operation are:-

» Inherent Fail Safe mode design in case of a power failure.

» UPS system with battery backup for 20 minutes to ensure safe completion of the ongoing wire wrapping, cutting crimping and welding cycle in case of power failure.

» No loss of data and positional information maintained to ensure continual operations.

» Live camera feed available to the operator to reset the operation manually if required.

» Embedded U-clips design in trays for holding and locking of wires and pins in proper position.

Corresponding author and email: Dr. P. S. Somayajulu (somaya@barc.gov.in)

Acknowledgement

The authors express their gratitude to Shri. Vivek Bhasin, Associate Director, Nuclear Fuels Group for his encouragement and support. The authors sincerely thank Shri. R. B. Bhatt and all colleagues at Fuel Fabrication Facility, Nuclear Recycle Board, Tarapur for their support and help extended. We also thank Shri. R. Rajakumar, Shri. B. N. Singh, Shri. G. Sivasankaran and the entire FRFCF team at Kalpakkam for their constant support and conducting the operation trials of the system.

References

1. H.S. Kamath, Recycle Fuel Fabrication Recycle Fuel Fabrication in India , IAEA TM , Fukui, Japan (**2008**).

2. Specification document for Mixed Oxide Fuel Pin. Document number- PFBR/31100/SP/1027.

3. Specification document for Stainless Steel Spacer Wire. Document number- PFBR/31130/SP/1011.

4. P.S. Somayajulu, K.V. Vrinda Devi, Rajashree Dixit, Prateek Pareek, Farman Ali, Madhusudan Sharma, R. Rajakumar, B.N. Singh and G. Sivasankaran, Non Contact Automated Inspection System for Wire Wrapped Fuel Elements, BARC Newsletter : 360 (**2017**).

Microbial Community Analysis of BARC Hospital Waste Water Treatment Plant Operating at Anushaktinagar

Bharati Pandey, Gagan D. Gupta, Subhash C. Bihani, Vinay Kumar
Radiation Biology & Health Sciences Division
Abhinandan Sharma
Technical Services Division, Bhabha Atomic Research Centre, Mumbai

Abstract

Deterioration of water quality contributes to water scarcity. The pollutants from several sources contribute to water pollution rendering the water unusable. Modern wastewater treatment plants across the world have adopted the Sequencing Batch Reactor (SBR) technology for the removal of organic matter and biological nutrients in the wastewater. Aerobic and anaerobic biological processes occur in sequential manner in a SBR plant in a single tank and technology offers significant advantage in terms of flexibility in handling low or varying influent load. The effectiveness of waste removal in SBR solely depends on the effective metabolism by microbial population present in the tank, which in turn affects settling rate of the sludge. High abundance of bulking and foaming bacteria can negatively impact SBR's performance and operation. The knowledge of filamentous bacterial population can facilitate better control and management of full-scale treatment plant. The culture-independent 16S rRNA metagenomics analysis of flocs from BARC hospital SBR was carried out by targeting hypervariable V3-V4 regions of 16S rRNA genes, with an aim to understand the capabilities of the plant. The approach successfully annotated 98.4% bacterial phyla. However, surprisingly, the load of each of the filamentous bacteria and archaea was not more than 1%.

Keywords: Wastewater treatment, Sequence Batch Reactor, bulking and foaming, bacterial identification, metagenomics, 16S rRNA sequencing

Introduction

Domestic sewage, industrial effluents, leachates from solid waste dumps and waste from farms such as pesticides, herbicides and organic manure, contribute to water pollution. Wastewater treatment plants across the world mostly use aerobic and anaerobic biological processes for the removal of organic matter and biological nutrients (Nitrogen and Phosphorous) in the wastewater. The principal application of the processes is for (1) the removal of the carbonaceous organic matter in wastewater, (2)nitrification, (3)denitrification, (4) phosphorus removal and (5) waste stabilization.

The Sequencing Batch Reactor (SBR) in a wastewater treatment plant works on the principle of fill-and-draw strategy and is based on sequential activated granular sludge process in which oxygen is supplied to facilitate the metabolic reaction (bacterial growth to break-down contaminants). The activated sludge (solid waste containing the bacterial colonies) is allowed to settle naturally under quiescent conditions. The settled sludge is partly removed for proper disposal and the rest is mixed with the next batch of wastewater. Recycling is necessary for activated sludge process. The key advantages of SBR process are: Dense microbial structure, good settleability, high biomass retention and the ability to tolerate high organic loading rate (Lili et al., **2005**). The effectiveness of waste removal in SBR depends on the effective metabolism by microbial population present in the tank. It has recently been suggested that the chemical composition, rather than the bacterial composition of the incoming wastewater, is the main factor in the formation of activated sludge structure (Shchegolkova et al., **2016**).

The bulking of sludge (improper settling) may arise due to (a) the growth of filamentous microorganisms (bacteria and algae), which do not allow desirable compaction; or (b) due to the production of non-filamentous highly hydrated biomass (Rao, **2007**). The presence of toxic substances in the influent, lowering of temperature and improper aeration are amongst the several well-known causes for spoiling the efficiency of SBR. These factors impair microbial growth and also change their population structure (Liu et al., **2008**).

It is important to study the composition of microbial community of the SBR tank and also their biodegradational capability for avoiding many technical problems. Various approaches have been used to identify microbial population in the activated sludge. Microscopy or conventional molecular methods may

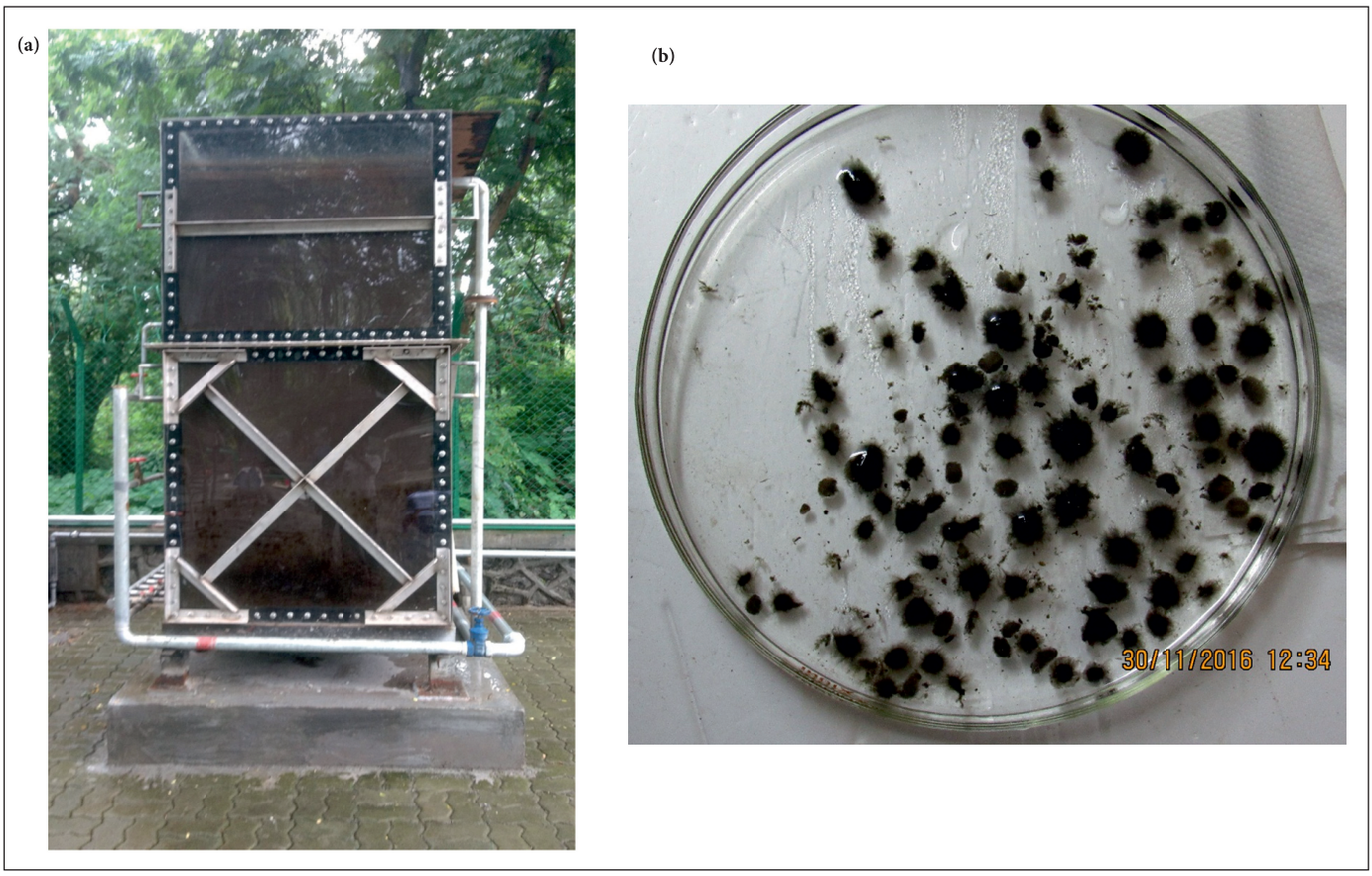

Fig.1. a)The SBR plant in Anushaktinagar, b) Granules structure

Table 1.

	pH	BOD (mg/ml)	COD (mg/ml)	TSS (mg/ml)	DO (mg/ml)	TN (mg/ml)
Influent	6.88	123.3	370.0	548.0	0.53	2.63
Effluent	6.73	23.3	70.0	76.0	2.05	0.93

not yield the full profile of bulking and foaming bacteria in the normal activated sludge (Guo and Zhang, **2012**). Importantly, 16s rRNA gene based metagenomic analysis is the most recent, cost-effective, and highly reliable microbial identification method based on Next Generation Sequencing (NGS) techniques (Forbes et al., **2017**). It is a culture independent technique and uses genetic material recovered directly from environmental samples (Liaw et al., **2010**).

In this paper, we present the bacterial community analysis of floc samples taken from SBR wastewater plant in Anushaktinagar, Mumbai. Some detailed information of the SBR is summarized in **Table 1** & **Fig. 1**.

To analyse the bacterial structure, total DNA was isolated and hyper-variable regions of V3 and V4 segments of 16S rRNA genes were PCR amplified. The amplicons were analysed using Miseq NGS. In total, we collected 94,883 sequence reads. In-house data analysis detected 28 phyla, 59 classes, 112 orders, 237 families, 583 genera, and 883 species.

Table 1. Characteristics of wastewater treatment plant; BOD, biological oxygen demand; COD, chemical oxygen demand; TSS, total suspended solids; DO, dissolved oxygen; TN, total nitrogen.

Materials and Methods

Sampling and DNA isolation

The samples were obtained from the wastewater treatment plant, Anushaktinagar, Mumbai. The treatment plant receives the wastewater generated from both domestic and hospital consumption. The samples were stored at -80°C. These samples were thawed on ice and centrifuged at high speed to harvest the microbial cells. The cell pellet was then re-suspended in DNA extraction buffer [50 mM Tris-HCl pH 7.6, 50 mM NaCl, 50 mM EDTA, 5% SDS, 1 mM DTT] (Roose-Amsaleg et al., **2001**). The cell lysis was supplemented by mechanical disruption using glass beads beating in tissue homogenizer for 2 minutes. The extracted DNA, present in solution form, was separated from cellular debris using centrifugation at 14000xg. The supernatant containing DNA was purified using phenol: chloroform extraction method followed by alcohol precipitation. The extracted DNA was checked for purity and integrity using 0.8% agarose gel

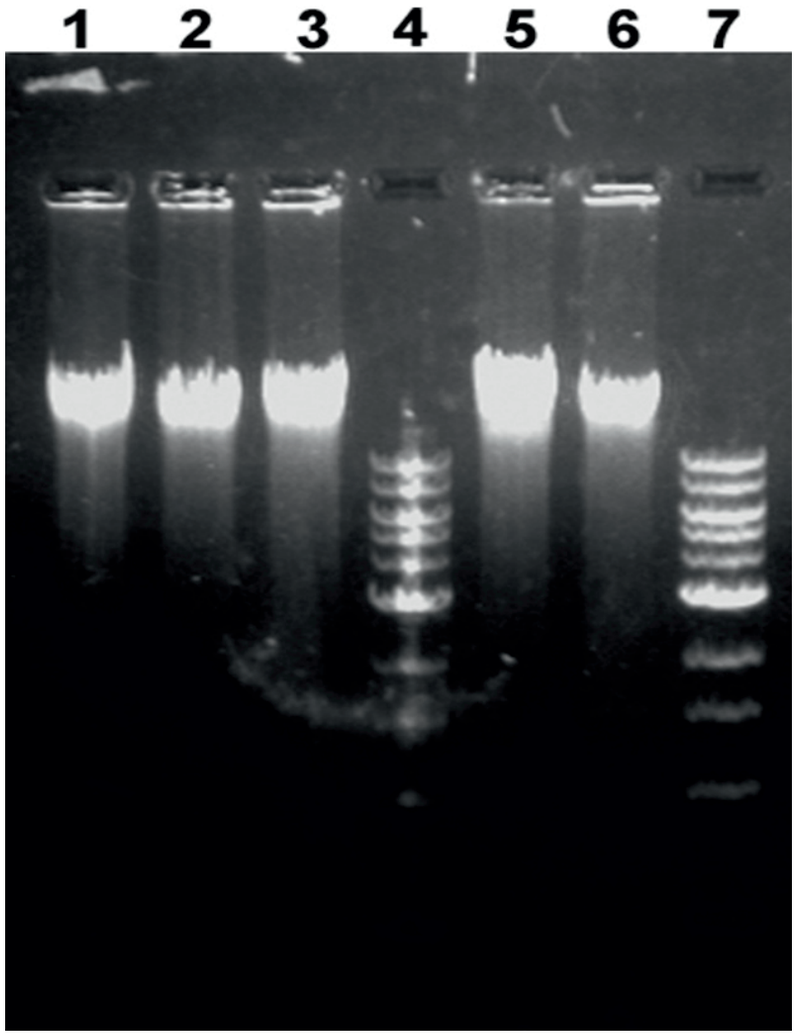

Fig. 2. Quality check of DNA extracted from microbial population of hospital SBR. Lane 1, Lane 2, Lane 3, Lane 5 and Lane 6 represents independent DNA extraction. Lanes 4 and 7 are DNA 1kb ladder.

electrophoresis (**Fig. 2**).

The cell lysis was supplemented by mechanical disruption (beating) in tissue homogenizer for a duration of 2 minutes by using glass beads.

Metagenomic Analysis

Variable regions V3-V4 of the 16S rRNA genes were amplified using universal primers of conserved regions. The PCR products were paired-end sequenced by Illumina Miseq platform (Illumina, San Diego, CA). A total 94,883 sequence-reads obtained in FASTAQ format were evaluated by FASTQC, using default parameters. The average read size was 301bp for forward and reverse sequences. All the sequences were analysed using Illumina BaseSpace application. The application performs taxonomy classification of individual 16S rRNA reads by using the Naïve-Bayesian based RDP classifier (Wang et al., **2007**) against Illumina-curated version of the GreenGenes taxonomic database. Abundances of the various taxa in a given sample were calculated as the total number of sequences assigned to a given taxa divided by the total number of sequences in that sample.

Results and Discussion

Bacteria present in wastewater treatment plants are important contributors in the degradation of organic and xenobiotic compounds present in the wastewater. Changes in the microbial diversity or metabolism of these bacteria can affect the whole wastewater treatment process (Guo et al., **2014**). However, despite their importance in the processes, microbial communities of these wastewater treatment plants are still poorly understood.

The taxonomic composition of SBR treatment plant was investigated at the levels of phylum, class, order, genus and species. The 16S rRNA metagenomics analysis of 94,883 reads successfully annotated 98.86% of total reads to the kingdom taxonomic level, including eubacteria (98.39%), viruses (0.44%) and archaea (0.03%). The microbial community structure of the sludge sample at the class, order and family level, each above 3.5% abundance level, are represented in **Fig. 3**. The microbial population of the sample was dominated by phylum Proteobacteria(61.42%), which is consistent with the earlier results of community analysis in the activated sludge samples (Xu et al., **2018).** Other significant microbial phyla were Bacteroidetes (15.48%), Firmicutes (6.66%), Planctomycetes (1.75%), Verrucomicrobia (1.57%), Actinobacteria (1.53%) and Acidobacteria (1.44%). Among Proteobacteria, Betaproteobacteria members were predominant at class, order and family levels, and were found to be most abundant in an earlier study as well (Shah, **2014**). Rhodocyclales, belonging to Betaproteobacterial class, was the most abundant order in the present microbial population (**Fig.3**). Members of the order "Rhodocyclales" comprise a group of bacteria which are involved in the removal of anthropogenic compounds in the environment (Loy et al., **2005**).

The present metagenomic analysis identified a large number of bacteria which are involved in the removal of pollutants from the SBR plant. Azospira, a nitrogen fixing bacteria from phylum Proteobacteria,

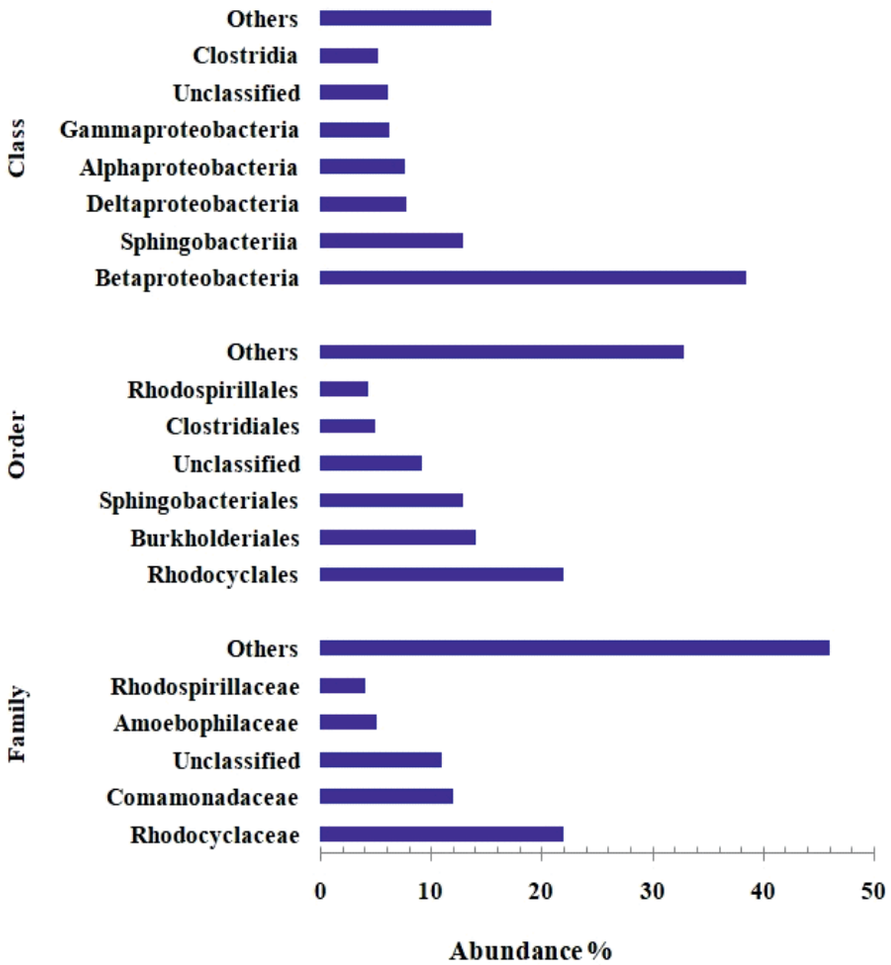

Fig. 3. Relative abundance of bacterial populations in the SBR plant. Unclassified sequences may be due to lack of reference sequences in the database.'Others' represent sum of all classifications with less than 3.50 % abundance.

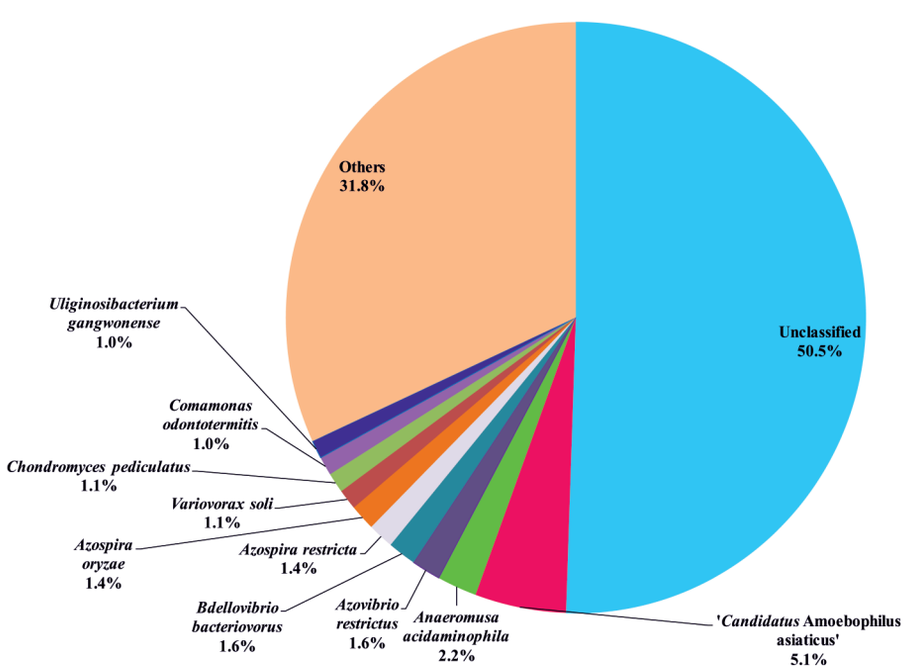

Fig. 4. Species level classifications of bacteria present in the sample. 'Others' represent sum of all classifications with less than 1 % abundance.

(**Fig. 4, Table 2**) was found to be the most abundantgenus. The Azospira strains, especially *Azospira oryzae*, have the ability to reduce perchlorate, nitrates and acytelyne (Bae et al., **2007**). Another highly prevalent species, Dechloromonas, has been suggested to be involved in de-nitrifying phosphate removal (DPR) in the anoxic periods in WWTPs (Terashima et al., **2016**). The DPR process, in comparison to the conventional enhanced biological phosphorus removal (EBPR) process, can reduce aeration demand and carbon source requirement. The species - *Bdellovibrio bacteriovorus* - is useful in the purification of wastewater as it decreases thegram-negative bacterial counts (Sockett & Lambert, **2004**). Several species of Magnetospirillum genus serve as denitrifying bacteria, degrade aromatic compounds under anaerobic conditions (Shinoda et al., **2005**).Likewise, members of Desulfovibrio genus are known as a sulfate reducing bacteria and possess the potential for bioremediation by anaerobic conversion of pollutants (Pires et al., **2006**).

The present study also reveals 'Candidatus Amoebophilusasiaticus' species as characteristic component of our SBR plant. This species has not been reported earlier in wastewater treatment plants and is an obligate intracellular amoeba symbiont (Schmitz-Esser et al., **2010**). Interestingly, we have found single floc-forming bacterial species, *Comamonas odontotermitis*, with nearly 1%abundance in SBR plant sample analysis. Although, species resolution was not very high (limited to less than 50%) in the present analysis, owing may be due to sequencing of only V3-V4 domains of 16S rRNA, several of identified species have also been observed in other metagenomics studies.

Table 2: Summary of the genus and species identified in the SBR sample

Taxonomy level	Classification	Relative abundance %	Characteristic features	Biological function	References
Genus	*Azospira*	8.84	Gram-negative, non-spore-forming, straight to curved rods with a single polar flagellum and harbor mostly nitrogen-fixing	Perchlorate and nitrate reducing bacteria. Key role in high nitrate removal efficiency in groundwater	Bae et al., 2007
	Dechloromonas	5.81	Facultative anaerobe, nitrate-reducing bacteria	Revealed strong ability to accumulate polyphosphate within its cells and leads to efficient in removal of phosphorus from wastewater	Terashima et al., 2016
	Candidatus Amoebophilus	5.08	Gram-negative, rod shaped	perform the decomposition of organic matter into methane and CO_2	Tsao et al., 2017
	Anaeromusa	2.24	Anaerobic gram-negative curved rods	Ferments and oxidizes amino acids	Baena et al., 1999
	Bdellovibrio	2.14	Gram-negative, obligate aerobic bacteria, highly motile, vibrio shaped, monoflagellated	Penetrate and lyses other gram-negative bacteria therefore useful in purification of wastewater	Sockett & Lambert, 2004
	Desulfovibrio	2.03	Gram-negative sulfate-reducing, rod-shaped, anaerobically growing bacterium	Reduces metals such as chromium (VI), manganese (IV), iron (III), technetium (VII), and uranium (VI) and alter their solubility and toxicity	Payne et al., 2002
	Magnetospirillum	1.99	Gram negative, helical, magnetotactic, microaerophilic spirillum	Used in the removal of heavy metals and radionuclides from waste water by magnetic separation	Yan et al., 2012
Species	*Candidatus Amoebophilus asiaticus*	5.08	Obligate endosymbiont		Choi et al., 2009
	Anaeromusa acidaminophila	2.21	Gram-negativeand obligately anaerobe	Amino acid degradation	Díaz et al., 2007
	Anaeromusa acidaminophila	2.21	Gram-negativeand obligately anaerobe	Amino acid degradation	Díaz et al., 2007
	Azovibrio restrictus	1.63	Gram-negative	Reductively dechlorinates tetra- and trichloroethene	Schlötelburg et al., 2002
	Bdellovibrio bacteriovorus	1.57	Predatory gram-negative, obligate aerobe	Biofilm degradation capacity and used for reducing fouling of membranes used for wastewater treatment	Özkan et al., 2018
	Azospira restricta	1.43	Rod-shaped, gram-negative	Nitrogen-fixing ability	Bae et al., 2007
	Azospira oryzae	1.41	Motile, facultative anaerobic and Gram-negative	Reduces selenate, perchlorate, nitrates and acytelyne	Hunter 2007
	Variovorax soli	1.12	Gram-negative, catalase- and oxidase-positive, rod-shaped, nonspore-forming, motile	Benzene degradation by a Variovorax sp. in a coal tar-contaminated groundwater microbial community	Posman et al., 2017
	Chondromyces pediculatus	1.10	Gram-negative, rod-shaped		Holt et al., 1989
	Comamonas odontotermitis	1.03	Gram-negative, aerobic, rod-shaped, motile	Floc-forming, isolated from various environments including soil, freshwater, wetland, activated sludge	Kim et al., 2008
	Uliginosibacterium gangwonense	1.0	Gram-negative, motile by a single polar flagellum		Weon et al., 2008

***Relative abundance =1%**

It has generally been observed that eubacteria dominated quantitatively over archaea in both domestic and industrial wastewater treatment plants. While ammonia-oxidizing bacteria are dominant nitrifiers, biological denitrification is driven typically by Methanisarcinales and Methanomicrobials archaeal groups during the anaerobic phase of the treatment plant. Surprisingly, archaeal load in the SBR was less than 1%.

In order to produce well-settling sludge, biomass flocs should be regular, dense and strong. Bulking and foaming are two major issues critical to proper functioning of wastewater treatment plants. Due to bulking, the flocs become less dense, which results in inadequate settling thereby causing serious problems in solid-liquid separation. Most of the bulking events are caused due to excessive growth of filamentous bacteria (Martins et al., **2004**). Foaming occurs mainly due to mycolata group of bacteria, many of which are also filamentous. The most commonly encountered bulking and foaming bacteria (BFB) belong to seven separate bacteria phyla (Nielsen et al., **2009**). Typically, Alphaproteobacteria ('Nostocoida'-like), Gammaproteobacteria (Thiothrix and type 021N), the Actinobacteria (Candidatus 'Microthrix', Mycolata) and Chloroflexi (types 1851, 0041 and 0092) species have been reported in high abundance in wastewater treatment plants (Guo and Zhang, **2012**). None of these BFB bacteria were found in high abundance (>1%) in the present study. Presently, active

research is ongoing to understand the identity and ecophysiology of filament morphotypes.

In our analysis, we observed high abundance of Comamonadaceae family (>10%) and order Burkholderiales (>12%). These have recently been suggested to be involved in the bulking process (Xu et al., **2018**). Further metagenomics analysis targeting V3-V4 and V6 hyper-variable domains of bacterial 16S rRNA and ITS1 and ITS2 regions of fungi, is being pursued for higher-order identification of microbe population. In addition to this, an overabundance of a filamentous fungi-like microorganism and certain nutritional conditions (nitrogen/phosphorus imbalance) promote bulking. Two successful filamentous bulking control mechanisms have been reported: 1) breakdown of filaments induced by collisions (physical cut) and 2) by decreasing the biomass loading rate (Matos et al., **2010**).

Corresponding author and email: Dr. Vinay Kumar (vinay@barc.gov.in)

Acknowledgement

We sincerely thank Shri K.N. Vyas, Chairman, Atomic Energy Commission, for his role in initiating these studies besides his continuous encouragement during the course of this study. We also thank Shri S.K. Jaiswal for his kind help with respect to wastewater treatment plant. We also thank Water Chemistry Division, Chemistry Group, BARC, who designed the first wastewater treatment plant functioning at IGCAR, Kalpakam. This facility provided the essential know-how and inspiration for the BARC SBR plant.

References

1. H. S. Bae, B. A. Rash, F. A. Rainey, M. F. Nobre, I. Tiago, M. S. da Costa and W. M. Moe, **2007**. International Journal of Systematic and Evolutionary Microbiology. 57:1521-1526.
2. S. Baena, M. L.Fardeau, T. H. Woo, B. Ollivier, M. Labat, and B. K. Patel, **1999**. International Journal of Systematic and Evolutionary Microbiology. 49:969-974.
3. S. H. Choi, M. K. Cho, S. C. Ahn, J. E. Lee, J. S. Lee, D. H. Kim and H. S. Yu, **2009**. The Korean journal of parasitology. 47:337-344.
4. C. Díaz, S. Baena, M. L. Fardeau and B.K.C. Patel **2007**. International Journal of Systematic and Evolutionary Microbiology. 57:1914-1918.
5. J. D. Forbes, N. C. Knox, J. Ronholm, F. Pagotto and A. Reimer, **2017**. Frontiers in Microbiology. 8: 1069.
6. F. Guo and T. Zhang, **2012**. Water Research. 46: 2772-2782.
7. J. Guo, Y. Peng, S. Wang, X. Yang and Z. Yuan, **2014**. Chemical Engineering Journal. 255:453-461.
8. J. G. Holt and S. T. Williams **1989**. Bergey's manual of systematic bacteriology. Vol. 4, Lippincott Williams & Wilkins.
9. W. J. Hunter, **2007**. Current Microbiology. 54:376-381.
10. K. H. Kim, L. N. Ten, Q. M. Liu, W. T. Im and S. T. Lee, **2008**. The Journal of Microbiology. 46: 390-395.
11. R. B. Liaw, M. P. Cheng, M. C. Wu and C. Y. Lee, **2010**. Bioresource Technology. 101:8323-8329.
12. L. Lili, W. Zhiping, Y. Jie, S. Xiaojun and C. Weimin, **2005**. Enzyme and Microbial Technology. 36: 487-491.
13. H. Liu, G. Li, X. Li and J. Chen, **2008**. Journal of Environmental Sciences. 20:1243-1249.
14. A. Loy, C. Schulz, S. Lücker, A. Schöpfer-Wendels, K. Stoecker, C. Baranyi, A. Lehner, and M. Wagner, **2005**. Applied and Environmental Microbiology. 71:1373-1386.
15. A. M. Martins, K. Pagilla, J. J. Heijnen and M. C. Van Loosdrecht, **2004**. Water Research. 38:793-817.
16. M. Matos, M. A. Pereira, A. Nicolau, A. L. Rodrigues, A. G. Brito and R. Nogueira, **2010**. In WEF/IWA Biofilm Reactor Technology Conference. pp.162-175.
17. P. H. Nielsen, C. Kragelund, R. J. Seviour and J. L. Nielsen, **2009**. FEMS Microbiology Reviews. 33: 969-998.
18. M. Özkan, H. Yılmaz, M. A. Çelik, Ç. Şengezer, E. Erhan and B. Keskinler, **2018**. Turkish Journal of Biochemistry. 43:296-305.
19. R. B. Payne, D. M. Gentry, Rapp-Giles, B. J., L. Casalot, and J. D. Wall, **2002**. Applied and Environmental Microbiology. 68:3129-3132
20. R. H. Pires, S. S. Venceslau, F. Morais, M. Teixeira, A. V., Xavier and I.A. Pereira, **2006**. Biochemistry. 45:249-262.
21. K. M. Posman, C. M. DeRito, and E. L. Madsen, **2017**. Applied and Environmental Microbiology. 83: e02658-02616.
22. C. L. Roose-Amsaleg, E. Garnier-Sillam and M. Harry, **2001**. Applied Soil Ecology, 18: 47-60.
23. C. Schlötelburg, C.von Wintzingerode, R. Hauck, F. von Wintzingerode, W. Hegemann, and Göbel, U. B. **2002**. FEMS Microbiology Ecology. 39:229-237.

24. S. Schmitz-Esser, P. Tischler, R. Arnold, J. Montanaro, M. Wagner, T. Rattei and M. Horn, **2010**. Journal of Bacteriology. 192: 1045-1057.

25. M.P. Shah, **2014**. Journal of Microbial and Biochemical Technology. S5:002-006.

26. N.M. Shchegolkova G.S. Krasnov, A. A. Belova, A. A. Dmitriev, S. L. Kharitonov, K. M. Klimina, N.V. Melnikova and A. V. Kudryavtseva, **2016**. Frontiers in Microbiology. 7:90.

27. Y. Shinoda, J. Akagi, Y. Uchihashi, A. Hiraishi, H. Yukawa, H. Yurimoto, Y. Sakai and N. Kato, **2005.** Bioscience, Biotechnology, and Biochemistry. 69: 1483-1491.

28. R. E. Sockett, and C. Lambert **2004**. Nature Reviews Microbiology. 2: 669-675.

29. M. Terashima, A. Yama, M. Sato, I. Yumoto, Y. Kamagata, and S. Kato, **2016**. Microbes and Environments. 31:449-455.

30. H. F. Tsao, U. Scheikl, J. M. Volland, M. Köhsler, M. Bright, J. Walochnik and M. Horn, **2017**. Scientific Reports. 7:3394.

31. Q. Wang, G. M. Garrity, J. M., Tiedje and J. R. Cole, **2007**. Applied and Environmental Microbiology. 73: 5261-5267.

32. H. Y. Weon, B. Y. Kim, S. H. Yoo, S. W. Kwon, S. J. Go and E. Stackebrandt, **2008**. International Journal of Systematic and Evolutionary Microbiology. 58:131-135.

33. S. Xu, J. Yao, M. Ainiwaer, Y. Hong and Y. Zhang, **2018**. BioMed Research International. doi: 10.1155/2018/8278970.

34. L. Yan, S. Zhang, P. Chen, H. Liu, H. Yin and H. Li, **2012**. Microbiological Research. 167: 507-519.

Eddy Current Based Process Vessel Inspection System

Debmalya Mukherjee, Shilpi Saha, S.G. Manral, Y. Chandra, S.B. Hande, S.K. Lahiri and P.P. Marathe
Control Instrumentation Division, BARC
Santanu Das and A.C. Bagchi
Integrated Fuel Fabrication Facility, BARC

Abstract

Non-destructive testing and evaluation (NDT&E) of process vessels is an essential exercise for the integrity management program of an industrial plant. In many cases, such vessels are never opened in their operational life time due to the presence of hazardous chemicals inside them. This calls for a non-invasive thickness estimation method to inspect zones of excessive thinning of vessel and estimate its possible life-span ahead. While various NDT&E techniques are suited for such applications like radiography, ultrasonic technique (UT), eddy current technology (ECT) etc, ECT has a specific advantage over other NDT techniques as it is sensitive to surface & sub-surface defects, can be automated, needs access to one side only with little or no surface preparation. ECT gives a volumetric estimation of thickness of the vessel, thereby reducing the time required for inspection. Keeping the above application constraints in mind, a hand-held ECT based thickness estimation system is developed and customized for inspection of Inconel-600 process vessels. The system is tested at BARC. The paper outlines the development of this system, testing and final validation.

Keywords: Handheld, Eddy Current, Thickness, Gauge, FPGA, Inspection

Introduction

Health monitoring of plant equipment is an essential and mandatory exercise to minimise plant down-time that affects its productivity and chances of accidental hazards. This becomes more critical for plants dealing with materials that are chemically hazardous in nature. While a variety of methods and associated systems exist for non-destructive testing and evaluation (NDT&E) of materials, they are mostly generic and needs to be customized to suit specific industrial equipment and environment. This poses a challenge to the integrity management program of the plant where in-situ inspection and periodic reporting is mandatory. One such activity is the inspection of process vessel for its overall thickness estimation. As the process vessels are not accessible from inside in their operational lifetime, it becomes essential to estimate its thickness with high degree of accuracy, to monitor (I) the gradual change in thickness over time and thereby, (ii) to estimate the life of the vessel before it can be replaced. There are various NDT&E techniques for thickness estimation of metals like, eddy-current testing (ECT), ultrasonic testing (UT) and radiography to name a few. Radiography needs access to both sides of the material [1] which is not feasible in the inspection of process vessels during plant operation. UT needs a surface treatment and application of couplant over the inspection surface.

ECT works on the principle of electromagnetic induction. In industrial scenario, among other electromagnetic non-destructive techniques like magnetic particle, magnetic flux leakage, magnetic Barkhausen emission, micromagnetic, potential drop, microwave, AC field measurement techniques etc., this technique finds large number of applications with respect to thickness estimation on conductive surfaces. ECT also finds versatile uses in power, aerospace and petrochemical industries. ECT shows excellent sensitivity to surface as well as sub-surface defects and doesn't require additional materials (couplant) between its sensors and material under inspection. In fact, ECT being an electromagnetic induction process, direct mechanical contact with the sample is also not required, as long as the sample is conductive. There are few commercially available ECT based inspection systems like NORTEC 600 [2], MINIMAC-50 [3] among others, but they are bulky and hence not suitable for on-site monitoring during plant operations. These constrains led to the development of a customized hand-held ECT based thickness estimation system.

The inspection system developed is used to estimate the thickness of Inconel-600 process vessels at Integrated Fuel Fabrication Facility (IF3), BARC. The nominal thickness of these vessels are 3mm. These vessels are never opened in their operational lifetime and must be

inspected regularly keeping safety and production down-time in mind. The handheld eddy-current based process vessel inspection system developed has a resolution of 100 microns. The system developed was calibrated and tested at bench-top with a reference plate of thickness varying in 100 microns steps. The instrument was thereafter used at different times over a year to inspect the same process vessel at IF3, BARC to ensure accuracy and repeatability.

The paper is organised as follows. Section 2 deals with the theory on ECT. Section 3 covers system and sensor development, signal analysis and calibration. Inspection of the process vessel and its validation is given in section 4. Section 5 concludes the work highlighting the major achievements and future scope of work.

Eddy current technology

Eddy current testing is based on the phenomenon of electromagnetic induction. An alternating current, when flowing through an eddy current test probe or sensing coil, generates an oscillating magnetic field. When the probe is brought close to a conducting material, a circulating eddy current is established through the material. Changes in material thickness or defects such as cracks, wall-thinning, corrosion metal loss, microstructure degradation leads to changes in the amount and pattern of these eddy currents and hence its induced magnetic field (secondary field). The interaction between primary field of sensing coil and secondary field generated by these eddy currents alter the sensor coil's impedance, Z. Z is a complex quantity, comprising of R the coil's resistance, and X_L the coil's inductive reactance. The relationship between Z, R and X_L is shown in equation 1.

$$Z = R + jX_L = R + j2\pi fL \qquad (1)$$

This impedance change, usually of the order of milli ohms to few ohms, (depending on the excitation current and frequency) is measured using high-precision bridge circuits, analysed and correlated with defect dimensions. To get sufficient eddy current field strength in the region of interest (inspection area) within the material, ferrite cores are used. In some applications, the secondary magnetic field is detected with separate receiver coil or a solid-state field detection sensors.

The eddy current density decreases exponentially with its depth inside the specimen, as shown in equation 2. J_x and J_0 are the eddy current densities at depth of x from the surface and on the surface respectively, while δ the standard depth of penetration [4].

$$J_x = J_0 e^{-x/\delta} \qquad (2)$$

Theoretical standard depth of penetration of eddy currents δ, is shown in equation 3.

$$\delta = 1/\sqrt{\pi f \mu \sigma} \qquad (3)$$

where is f is excitation frequency, μ and σ are respectively the magnetic permeability and electrical conductivity of the specimen. The knowledge of δ allows designers to choose excitation frequency appropriately based on the material under inspection.

When an ECT probe is brought in close proximity of a conducting non-ferromagnetic material, its inductive reactance decreases while its resistance increases. The inductive reactance decreases due to increase in

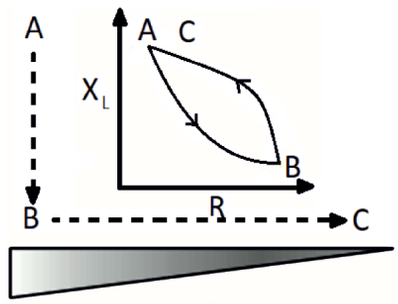

Fig. 1. The locus of coil impedance when it is brought close to a conductive surface of varying thickness

strength of secondary field (opposing the primary field) reducing net effective primary field, thereby reducing the coil's apparent inductance. As more energy is being dissipated due to induction of current in the specimen, the coil's apparent resistance goes up. The combined effect of change in X_L and R, alters the impedance Z of the coil. In most cases, it is the locus of Z that is monitored to get an estimate of the health of the material under inspection. The locus of $Z = R + jX_L$ for thickness reduction in a material is shown in **Fig. 1**, for sensor positions marked as A, B and C. As the sensor moves from A to B, i.e. from air onto the material surface, electromagnetic coupling between the coil and material goes up, increasing the eddy current in the material, thereby increasing the energy dissipation (increase in R) and secondary field opposing the primary field (decrease in X_L). As the sensor is moved over the material from B to C, the net volume of the material below the sensor goes down, reducing the net eddy currents generated in the specimen, thus decreasing energy

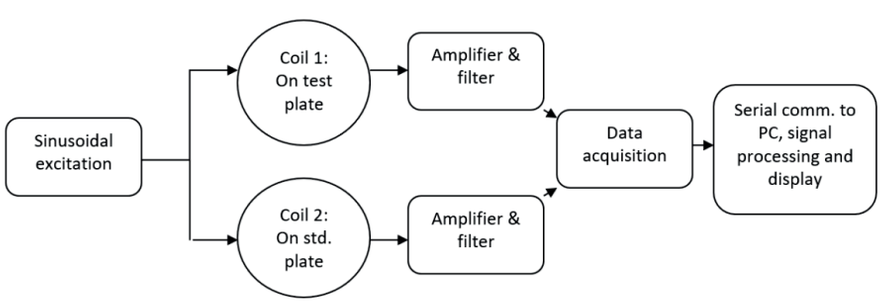

Fig. 2. Schematic block diagram of EC based thickness measurement system

dissipation (decrease in R) and thereby, reducing secondary field strength leading to increase in X_L. As the order of R is much less than that of X_L, reduction in thickness leads to a monotonic increase of Z, which is sensed by the system developed and calibrated against material thickness. More details on this technology can be found in [5].

System development and signal analysis

The ECT system was designed to measure and report thickness of 12" Inconel-600 vessels of nominal thickness 3mm. The inspection range is set at 2.5mm to 3mm. Thickness below 2.5mm is considered unsafe by the user and is classified accordingly by the system as unsafe zones irrespective of its absolute thickness. The system is designed to have 2 independent sensors having identical sinusoidal excitation. One sensor is for thickness measurement (Sensor 1) while the other is kept over a reference plate of the same material seeing the same ambient condition (Sensor 2). The purpose of such a design is to negate temperature bias and eliminate pick-ups due to common mode effects.

System development

The schematic block diagram of the system developed is shown in **Fig.2**. Two identical coils made of super enamelled, copper wire is wound around a ferrite core, and is excited by a sinusoidal constant current source. The frequency is set such that strength of eddy currents at the inside surface of vessel (3mm) is at least 50% of that of the surface currents, by inserting the appropriate parametric values (μ and σ) in equation 2 & 3. Each sensor is connected to the circuit board with high quality microwave shielded-coaxial cable (RG-178), to maximize noise immunity. These cables have a highly

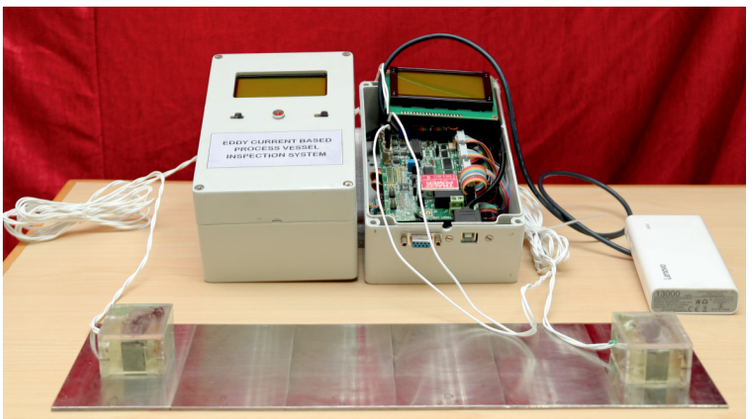

Fig. 3. Handheld EC based thickness measurement system with calibration plate, battery and sensors

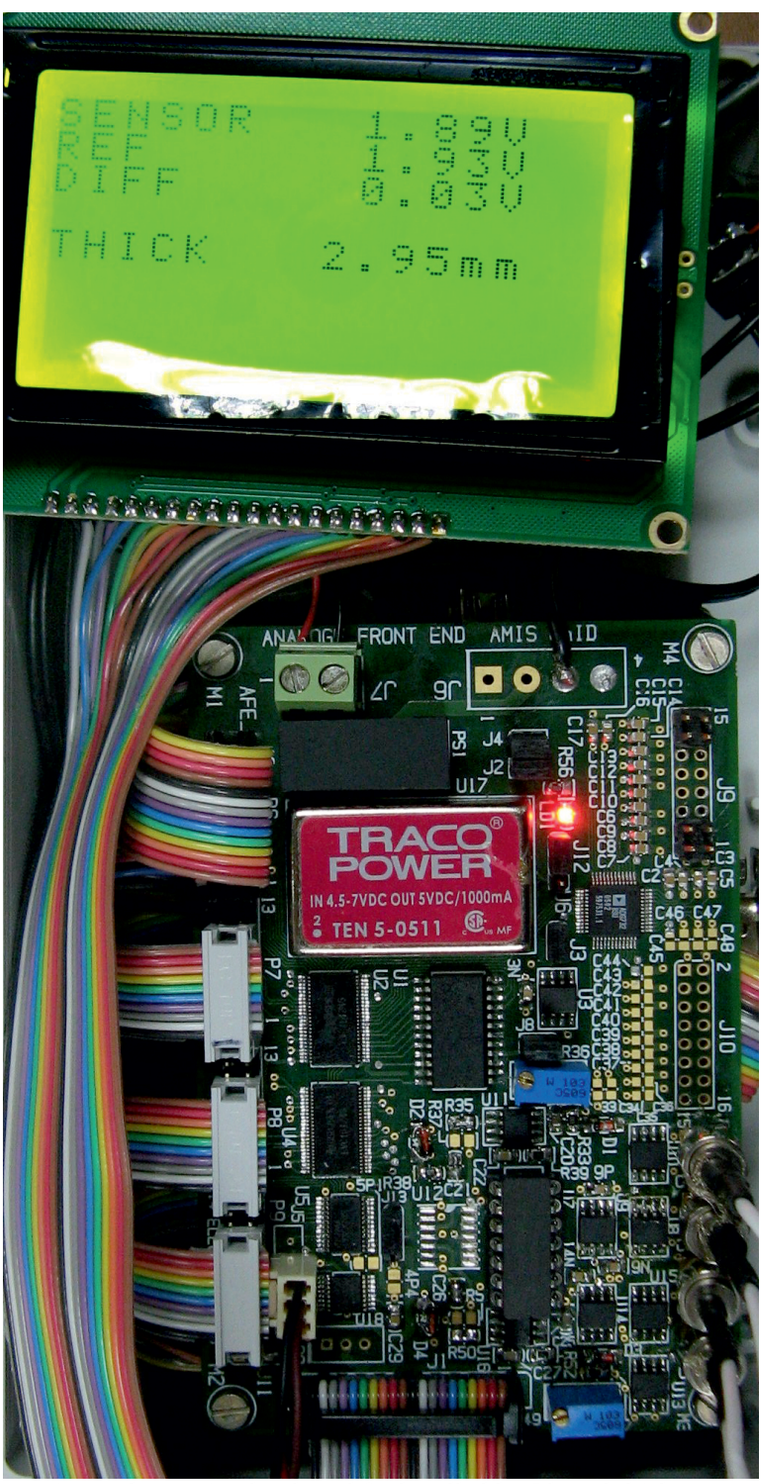

Fig. 4. Electronics developed for handheld EC based thickness measurement system

stable dielectric and low capacitance.

The sinusoidal signal obtained from an oscillator circuit is fed to a voltage-to-current (V-I) converter circuit. This in turn excites the sensor coils with a constant sinusoidal current source, $I(t)=I_0 \sin(2\pi ft)$, where constants I_0 and f are decided based on inspection parameters. Voltage drop across either of the coil is given in equation 3.1 and 3.2.

$$V = L\,dI(t)/dt + RI(t) \qquad (3.1)$$

$$V=2\pi fLI_0\cos(2\pi ft)+RI_0\sin(2\pi ft) \qquad (3.2)$$

The voltage signal obtained from each coil is subjected to analog signal conditioning, which involves envelop detection, level translation and denoising. They are thereafter sampled at 100Hz using custom built low power FPGA based data acquisition system. The system is powered by a rechargeable battery (portable cell-phone charger). It is fitted with an LCD display to show thickness in mm and a serial communication link with PC for calibration, graphical display (GUI), signal analysis and grid-array inspection.

After digitization, the conditioned signal from both sensors are observed by keeping sensor 1 ($V_1(t)$) over 3mm plate and sensor 2(V_2) over a standard plate. At this condition, a 'Zeroing' (bias switch) is set, which initializes and subtracts a bias such that the difference between sensor 1 & 2 goes to 0V (equation 4) for 3mm specimen thickness. V_2 and bias is not allowed to change throughout the length of the inspection and must be re-initialized at every power-on. The difference between signals of $V_1(t)$ and V_2 along with bias correction ensures that output reads 0V for 3 mm thickness.

$$V_0(t) = V_1(t) - V_2 - bias \qquad (4)$$

At 3mm, sensor 1 is at position B of **Fig.1**. It can be seen that as the thickness of material below sensor 1 reduces, the Z of the coil goes up. Since, the sensor is being excited by a constant current, $V_1(t)$ goes up. Other parameters of equation 4 being constant, $V_0(t)$ goes up. Thus $V_0(t)$ is 0V when sensor 1 is over 3mm thick material and monotonically increases as the material thickness decreases. This $V_0(t)$ is used to calibrate the ECT system. The handheld system with sensor and calibration template is shown in **Fig.3** and associated electronics in **Fig.4**.

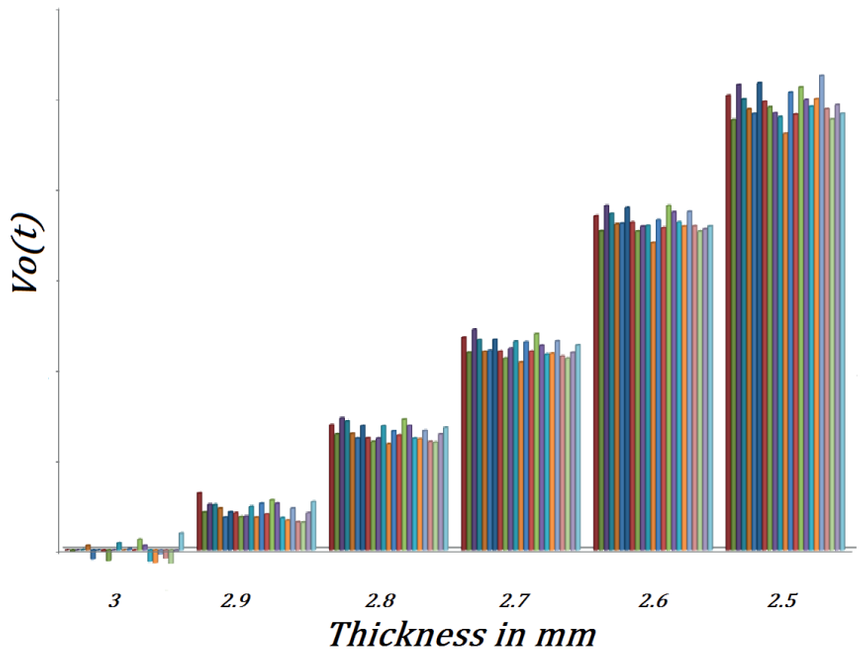

Fig. 5. Data of accuracy and repeatability tests for the thickness measurement system over calibration template.

Calibration and table-top validation

The system is calibrated with an Inconel-600 template having 3mm, 2.9mm, 2.8mm, 2.7mm, 2.6mm and 2.5mm standard thicknesses, with a tolerance of 10 microns. After securely fastening sensor 2 to a reference plate, the system is switched on with sensor 1 over 3mm calibration template. The bias correction is done ('Zeroing'), and $V_0(t)$ becomes 0 for 3mm. Sensor 1 is then moved over the calibration template and $V_0(t)$ is observed for each thickness. The process is repeated several times to establish the repeatability of the sensing system (**Fig.5**). The variance observed for each thickness template was in the order of 0.2 mV. With a set of such readings available, a least square curve fitting algorithm was used to map the recorded $V_0(t)$ to a typical thickness value.

Vessel inspection and verification

The inspection vessel of 12" diameter, was divided into 12 zones, which in turn was sub-divided into smaller grids. Each grid has the same dimension as that of the sensor. The calibrated system is switched on and connected to a laptop. Sensor 2 is placed on the reference plate. A GUI receives the signal from ECT system and displays the signal values from sensor 1, 2 and their difference. The zone is selected from a drop-down menu and each grid is marked as a button on the GUI. The analyst has to select which zone and click on grid number after placing sensor 1 over the designated area of the vessel. This operation automatically records the voltage levels of sensor 1 & 2, and files it for later analysis. During the entire operation, the LCD on the ECT system continues to display the estimated vessel thickness in real

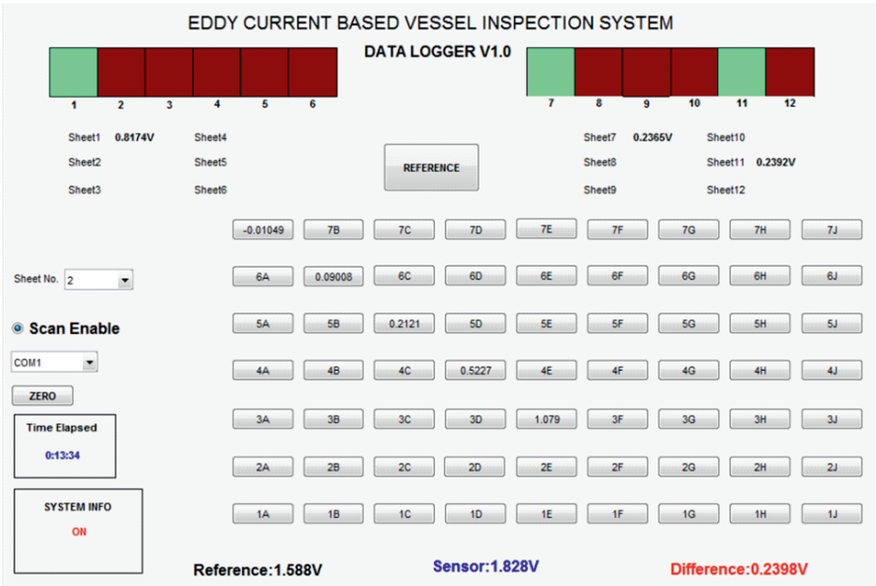

Fig. 6 A snapshot of the GUI during vessel inspection

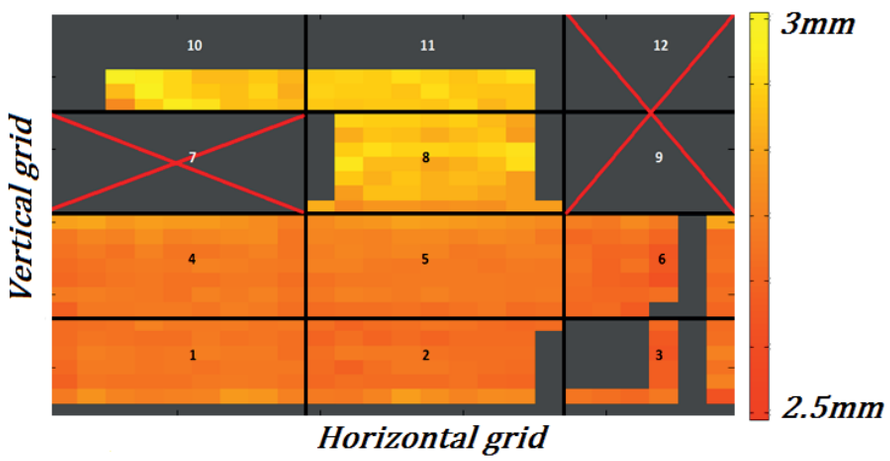

Fig. 7. Heat map of vessel thickness generated post

time. A snapshot of the GUI is shown in **Fig.6.**

As the analyst completes one zone, it gets highlighted with a different colour. After completing all the zones, a 'generate report' function can be used to analyses all the data collected against the predetermined calibration curve. The analysis software finally creates a heat map of the vessel surface (**Fig.7**) and a spreadsheet with thickness estimates of each grid in mm.

It takes approximately 1.5 to 2 hours to inspect a vessel and generate its thickness report.

Post inspection and analysis, the vessel was subjected to spot measurements with ultrasonic thickness gauge for verification. The difference was found to be less than 30 microns. The same vessel was inspected multiple times throughout the year to establish repeatability of the developed system.

Conclusion

The handheld ECT system is a fast and convenient way to estimate thickness of non-ferromagnetic conductive materials. It has a specific advantage to inspect the equipment in plants that are difficult to access. The system will now be calibrated to measure vessel thickness of other materials, with an inbuilt library to load calibration file of the selected material. In future, this system will be integrated with other NDT sensors to develop a more comprehensive hand-held inspection tool.

Corresponding author and email: Shri Debmalya Mukherjee (debmukh@barc.gov.in)

Acknowledgement

The authors are grateful to Shri D. Das, AD (E), E&IG for his encouragement and support in pursuing specialised NDT applications being developed for BARC and other DAE units. The authors are thankful to user division IF3, BARC for their extensive support during inspection trials and system validation.

Reference

1. Jasinien E, Raiutis R, Iiteris R, Voleiis A, Vladiauskas A, Mitchard D & Amos M, Insight- Non-Destructive Testing and Condition Monitoring, Vol 51 (9), **2009**, pp 477-483.

2. NORTEC 600 Eddy Current Flaw Detector, Performance and Innovation in Eddy Current, **2017**, Olympus, https://www.olympus-ims.com/en/nortec 600

3. MINIMAC 50, Magnetic Analysis Corp., 2018, https://www.mac-ndt.com/wp-content/uploads/**2018**/08/MINIMAC-50-COMPLETE-2.pdf

4. Cecco VS, Vandrunen G &Sharp FL, Eddy current testing - Manual on eddy current method - Vol 1, ChalkRiverNuclearLaboratories, Atomic Energy of Canada Limited, Nov **1981**.

5. Donald J. Hagemaier, Fundamentals of Eddy Current Testing, ASTN, ISBN 0-931403-90-1, **1990**

परमाणु ऊर्जा के लिए नए पदार्थों का विकास

डॉ. जी. के. डे
पदार्थ वर्ग, भापअ केंद्र, ट्रांबे – 400085

प्रस्तावना

परमाणु रिएक्टरो में विभिन्न प्रकार के पदार्थों का प्रयोग किया जाता है । इन पदार्थों को उपयोग के आधार पर वर्गीकृत किया जा सकता है । उदाहरण के लिये नाभिकीय ईंधन के तौर पर विकसित पदार्थ जैसे यूरेनियम, थोरियम इनके ऑक्साइड्स, न्यूट्रॉन शोषक पदार्थ जैसे बोरोन, बोरोनकार्बाइड, संरचनात्मक पदार्थ जैसे जर्कोनियम, लोहा एवं निकल पर आधारित सम्मिश्र एवं बेरिलियम धातु जिनका प्रयोग विभिन्न नाभिकीय कार्यक्रमों में किया जाता है।

विकासमान स्वदेशी नाभिकीय ऊर्जा निकायों के लिये पदार्थ, प्रक्रियाओं एवं फ्लो शीट के विकास के अंतर्गत निम्नलिखित प्रक्रियाओं को कार्यान्वित किया गया है –

१. आधुनिक न्यूक्लियर रिएक्टर एवं विशिष्ट उपयोगों के लिये सम्मिश्र, सिरेमिक्स, विलेपनों में प्रगत पदार्थों एवं प्रौद्योगिकी का विकास,

२. स्वदेशी संसाधनों से धातुओं के निष्कर्षण हेतु प्रक्रियाओं का विकास

३. रिफ्रैक्टरी एवं रेयर अर्थ स्रोतों से धातुओं की प्राप्ति,

४. सूक्ष्म संरचना (माइक्रो स्ट्रक्चर) एवं रूप परिवर्तन का अध्ययन,

५. परमाणु ऊर्जा विभाग इकाइयों को पदार्थों के डिजाइन, उत्पादन एवं प्रचालन में सहायता देना, पदार्थों के नाकाम होने के कारणों का पता करना एवं निदान खोजना,

६. नाभिकीय क्षेत्र में पदार्थों को चुनाव के लिये परखना, प्रयुक्त पदार्थों का संक्षारण (कोरोज़न-जंग) अध्ययन एवं समस्याओं का निदान / सुधार ।

मुख्यत: जिन पदार्थों का विकास अपने विखंडन कार्यक्रम के लिये किया गया है, वह हैं:

१. न्यूक्लियर ईंधन पदार्थ – यूरेनियम, थोरियम, सम्मिश्र, यूरेनियम ऑक्साइड, मिश्रित ऑक्साइड ईंधन ।

२. न्यूट्रान शोषक पदार्थ–बोरोन, बोरोनकार्बाइड, रिफ्रैक्टरी एवं रेयर अर्थ धातु बोराइड।

३. संरचनात्मक पदार्थ –जर्कोनियम, नियोबियम, वैनेडियम एवं मिश्र धातु, इस्पात, सुपर- मिश्रधातु ।

४. अन्य नाभिकीय उपयोग–सिलिकॉन कार्बाइड, बेरिलियम, कोबाल्ट, न्यूट्रान सेंसर, लेड-बिस्मिथ, लेड-लिथियम सीलेंट, धात्विक कांच, उच्चताप अतिसुचालक (सुपरकंडक्टर) नमूना मोटर, विद्युतधारा प्रति बंधक यंत्र अन्य उपयोग - आकार स्मृति (शेप मेमोरी) मिश्र धातु, ईंजीनियरिंग उपयोगों हेतु डिजाइन एवं विकास, बेरिलियम घटक, ठोस आक्साइड ईंधन सेल घटक ।

केवल नाभिकीय कार्यक्रम के ही नहीं अपितु बहुत से ऐसे पदार्थों का विकास इसलिए किया गया कि उनका उपयोग कर समाज के विभिन्न वर्गों के लोग इससे लाभान्वित हों । इनमें से कुछ ऐसे हैं जो चिकित्सा एवं उपचार में प्रयोग होते है । इसी तरह राष्ट्रीय सुरक्षा में उपयोग के लिए उपयुक्त पदार्थों के अलावा पदार्थों से जुड़ी कई तरह की प्रक्रियाएं जैसे उनको जोड़ने की विधि,उन पर विभिन्न प्रकार की परतें डालने की विधि ताकि वे विषम परिस्थितियों का सामना बेहतर तरीके से कर सकें ।

हमारे भारतीय परमाणु बिजली घरों में जिन पदार्थों का प्रयोग किया गया है वह पूरी तरह से स्वदेशी हैं। किसी भी पदार्थ को बनाने के लिए पहले उसके अयस्क की खोज की जाती है । उसके बाद उस अयस्क को खनिज ड्रेसिंग और सान्द्रता की प्रक्रिया से गुज़ारा जाता है, इसके उपरान्त धातु निष्कर्षण किया जाता है यानी उसका धातु में रूपांतरण होता है । इस प्रक्रिया के दौरान जो अपरिष्कृत धातु मिलती है उसे परिष्कृत करके शुद्ध धातु बनायी जाती है । यह प्रक्रिया लगभग सभी धातुओं को बनाने में प्रयुक्त की जाती है । हम अपने परमाणु बिजली घरों में जिन धातुओं का प्रयोग करते हैं उनमें से अधिकतर धातुओं का उत्पादन भारत में ही किया जाता है । हम धातु उत्पादन में स्वावलंबी हैं ।

ये उन सभी धातुओं की एक सूची है,जिनका हमने सफलता पूर्वक अपने अयस्कों से निर्माण करने की विधि को स्थापित किया है । भारतीय अयस्कों से इन धातुओं के निष्कर्षण के लिए प्रौद्योगिकी विकसित की गई। इनमें से कुछ धातु हैं-

- टाइटेनियम(Ti)
- जर्कोनियम (Zr)
- वैनेडियम (V)
- टंगस्टन (W)
- नियोबियम (Nb)
- यूरेनियम (U)
- थोरियम (Th)

धातुओं का प्रयोग शुद्ध रूप में नहीं किया जाता है । उनका प्रयोग मिश्रधातु के रूप में किया जाता है । इसी लिए मिश्र धातु के विकास की आवश्यकता होती है । मिश्र धातु का विकास तीन प्रकार से किया जाता है ।

१. प्रमाणित धातु का परीक्षण करके उसका पुन:निर्माण करना -

ऐसा करने के लिए हमें उस आयातित मिश्र धातु का संघटन सूक्ष्म-संरक्षण, बनावट और ठोस घनत्व की जानकारी की आवश्यकता होती है । इन सभी जानकारियों को हासिल करने में हम सक्षम हैं । हमारे पास वह सभी उपकरण हैं जिनका प्रयोग करके हम ये सारी जानकारियां हासिल कर सकते हैं । जिसके फलस्वरूप हम प्रमाणितधातु का निरीक्षण करके उसका अपने देश में पुन:निर्माण कर सकते हैं।

२. जिन मिश्र धातुओं का हम नमूना प्राप्त नहीं कर सकते हैं पर हमारे पास उन मिश्र धातुओं की जानकारी उपलब्ध है और इन जानकारियों के आधार पर हम उन सम्मिश्रणों को बना सकते हैं और ऐसा करने में भी हम पूरी तरह से सफल रहे हैं ।

३. हम अपना स्वयं का भारतीय सम्मिश्रण तैयार करना चाहते हैं। इसमें दो विधियां हैं:

(अ) प्रयोगात्मक विधि : इस विधि में हम लगभग ५००-६०० सम्मिश्रण बना सकते है जिसमें से एक सम्मिश्रण हमारे उपयोग को लिए पर्याप्त होगा ।

(ब) संघनित, प्रारम्भिक सिद्धांत : इसमें हम सैद्धांतिक आधार पर उस सम्मिश्र की कल्पना करें जो हमारे लिए उपयुक्त होगा, मजबूती की दृष्टि से और जहां उपयोग होगा वहां के वातावरण की दृष्टि से, फिर उस सिद्धांत के आधार पर हम एक ही सम्मिश्र को बनाएं, जो हमारे अनुप्रयोग के लिए उपयुक्त हो।

किसी भी सम्मिश्र को बनाने के बाद उसका गलन करते है, गलन और ढलाई के बाद विभिन्न प्रकार के मध्यवृत्ति ताप से उसका उपचार किया जाता है और

अंत में अंतिम प्रसंस्करण होता है । उत्पाद वांछित आकार के साथ साथ वांछित सूक्ष्म संरचना, टेक्स्चर और उपयुक्त घनत्व के साथ होना चाहिए । निर्माण के प्रत्येक चरण में सूक्ष्म संरचना और टेक्स्चर का परीक्षण करना आवश्यक है और इन सभी परीक्षणों के लिए हमारे पास उपयुक्त उपकरण मौजूद हैं। मिश्र धातु के विकास के लिए कई तरह के उपकरण की आवश्यकता होती है । माइक्रो स्ट्रेक्चर यानी सूक्ष्म संरचना को परखने के लिए हम तरह-तरह के सूक्ष्मदर्शी यंत्रों यानी माइक्रोस्कोप का प्रयोग करते हैं । जैसे ऑप्टिकल माइक्रोस्कोप, स्कैनिंग इलेक्ट्रान माइक्रोस्कोप, ट्रान्समिशन इलेक्ट्रॉन माइक्रोस्कोप । इस क्षेत्र में भा.प.अ. केंद्र, आई. आई. टी. एवं टी. आई. एफ. आर. की सम्मिलित क्षमता बहुत अधिक है। उदाहरण के लिए सर्वोच्च विभेदन इलेक्ट्रॉन माइक्रोस्कोप सर्वप्रथम टी.आई.एफ.आर., मुंबई में लगाया गया, जो वहां पर कार्यरत है और हमारे अनुसंधानों में उसका उपयोग किया जाता है । इसी प्रकार मैकेनिकल परीक्षणों की सारी सुविधाएं भा.प.अ. केंद्र में उपलब्ध हैं और यह हमारे भारतीय सम्मिश्र धातुओं के विकास में बहुत सहयोग करता है । संक्षारण, गुणों का मूल्यांकन करने की क्षमता हममें है । सम्मिश्र पर विकिरण या किरणन का अध्ययन करना भी हमारे लिए आवश्यक है और इसमें हम सक्षम हैं ।

नाभिकीय ईंधन पदार्थ में हमने जो विकास किया है उनमें यूरेनियम, थोरियम, यूरेनियम ऑक्साइड, मिश्रित ऑक्साइड ईंधन प्रौद्योगिकी एवं प्रोसेसिंग फ्लोशीट, यूरेनियम अयस्कों का जादूगूडा, तुरामडीह कारखाने में प्रौद्योगिक (प्रोसेसिंग), अनुसंधान रिएक्टर के लिए यूरेनियम प्रौद्योगिक कारखाने और उनका विकास, पारंपरिक तथा अपारंपरिक स्रोत से यूरेनियम तथा अन्य पदार्थों की प्राप्ति के लिए विभिन्न फ्लोशीट का भी विकास किया गया है । भारतीय अयस्कों से यूरेनियम तथा अन्य पदार्थों अथवा खनिजों को निकालने के लिए विभिन्न पद्धतियों का विकास किया गया है ।

तुमलापल्ली और मेघालय में यूरेनियम के भंडार का पता चलने के बाद इनसे यूरेनियम के निष्कर्षण का काम पहले तुमलापल्ली में शुरु किया गया । स्वदेशी अयस्कों से यूरेनियम धातु के निष्कर्षण का कार्य औद्योगिक परिमाण में तेजी से किया जा रहा है । इसके लिए प्रयोग शाला में छोटे पैमाने पर शोध के द्वारा विकसित विधियों को बड़े पैमाने में उपयोग करने का काम किया जा रहा है ।

ऊष्मा उपचारित पदार्थ क्षेत्र में, इसके लिए जर्कोनियम, नियोबियम, वैनेडियम एवं उनके समिश्रों का ऊष्मा उपचारित इस्पात, सुपर मिश्र धातु इत्यादि का विकास किया गया है। इनके उत्पादन प्रक्रम इसमें शामिल है । ईंधन ट्यूब के लिए जिरकोलाय, कैलेंड्रिया नलिका,जर्कोनियम नियोबियम प्रेशर नलिका, जर्कोनियम नियोबियम कॉपर गाटर स्प्रिंग का निर्माण भी भारत में किया गया है । एल.डब्ल्यू.आर. के लिए प्रेशर वेसेल इस्पात, एफ.बी.आर. के लिए इस्पात का विकास किया गया है । प्रगत नाभिकीय रिएक्टरों के योग्य उच्च ताप सह धातु, मिश्र धातु एवं स्टील पर एलूमिनाईड एवं सिलिसिडाइट कोटिंग का विकास किया गया है। जर्कोनियम सम्मिश्र जंग रहित इस्पात प्राथमिक उष्मान्तरण नलिका (स्टेनलेस स्टील प्राइमरी हीट ट्रान्सफर पाइपिंग) का विभंजन एवं फटीग अध्ययन किया गया है । नियोबियम-१,जर्कोनियम-०.१ कार्बन सम्मिश्र, टीजेडएम पदार्थ, उनके फ्लोशीट का विकास एवं विकृत (डिफॉरमेशन) व्यवहार, संरचना गुण-धर्म संबंध का भी अध्ययन किया गया है ।

· मिश्र धातु विकास के कुछ उदाहरण

I. नियोबियम- १, जर्कोनियम- ० . १ कार्बन सम्मिश्र : इस सम्मिश्र को पहले चरण में इलेक्ट्रान किरण द्वारा गलित किया जाता है, फिर दूसरे चरण में इसका वैक्यूम (निर्वात) आर्क रीमेल्टिंग किया जाता है । उसका ऊष्मा उपचार करने के बाद उसे एक आकार दिया जाता है उसके बाद उसको गर्म करके सामान्य तापमान पर उसके शेष आकार को बनाया जाता है । यह उदाहरण एक ऐसे सम्मिश्र का था जिसको कांपैक्ट हाई टेम्परेचर रिएक्टर में इस्तेमाल किया जाएगा । इसी पद्धति की रुप रेखा को अपनाते हुए कई अन्य पदार्थों का विकास किया गया है ।

II. एक्सिलिरेटर ड्रिवेन सुपर क्रिटिकल सिस्टम, एडवांस हेवी वाटर रिएक्टर जैसे कई तरह के जटिल संयंत्रों के निर्माण के लिए जिन पदार्थों की आवश्यकता होती है उसका विकास किया गया है । उदाहरण के लिए ग्रेफाईट शीतलक ट्यूब, रिएक्टर धातु ऍलाय, बेरीलियम ऑक्साईड, लेड बिस्मिथ शीतलक, ऊष्मा उपचारित जर्कोनियम ऍलाय का विकास, ट्राईसो कोटिंग इत्यादि । ट्राईसो कोटिंग के द्वारा सुरक्षा में वृद्धि होती है, विखंडित पदार्थ लेपित नली कणों के अंदर ही रहते हैं, जिससे ज्यादा बर्नअप मिलता है ।

शेप मेमोरी (आकार स्मृति) मिश्र धातु का निर्माण: इन मिश्र धातुओं में पूर्व आकार को याद रखने की क्षमता होती है और इस क्षमता के कारण इनका प्रयोग कई महत्वपूर्ण स्थानों पर होता है । इस सम्मिश्र का विकास भा.प.अ. केंद्र में किया गया है । इस पद्धति की जानकारी एडीए (एयरक्राफ्ट डेवलपमेंट अथॉरिटी) को दी गयी है, जिसके आधार पर उन्होंने बंगलुरु में एक कारखाना बनाया जिसमें इसका निर्माण बड़े पैमाने पर किया जा सकता है । इसमें बने आकार स्मृति मिश्र धातु निकिल टाईटेनियम का प्रयोग भारत में निर्मित हल्के लड़ाकू विमान, (लाईट कॉम्बैट एयरक्राफ्ट) तेजस में किया जाता है ।

संलयन कार्यक्रम के लिये पदार्थ

पहले कुछ उद्धरण विखंडन ऊर्जा द्वारा उत्पन्न कार्यक्रमों में प्रयोग किए जाने वाले पदार्थों के बारे में दिए गए हैं । अब कुछ ऐसे पदार्थों का उल्लेख किया जा रहा है जिनका उपयोग संलयन ऊर्जा के विकास में होगा । इनमें एक महत्वपूर्ण उपलब्धि रिड्यूस्ड एक्टिवेशन फेरिटिक मॉर्टेन्सिटिक स्टील के विकास की है जिसका निर्माण भारत में किया गया है । इस पदार्थ का बहुत बड़े पैमाने पर उत्पादन किया जाएगा। इस इस्पात का उपयोग ६२३-८२३ डिग्री सेल्सीयस पर किया जायेगा । इसका निम्न तापमान इसलिए रखा गया है जिससे विकिरण प्रेरित भंगुरता (रेडिएशन इंड्यूस्ड ईमब्रिटलमेंट) कम हो । इसके उच्च तापमान का निर्धारण इसके ताप सहन क्षमता को ध्यान में रखते हुए किया गया है । इस इस्पात का विकास एक अन्य इस्पात के आधार पर किया गया है जो संशोधित ९ Cr-१ Mo इस्पात है इसमें Mo को W द्वारा विस्थापित किया गया है और Nb को Ta द्वारा विस्थापित किया गया है । इसका उद्देश्य है विकिरण के स्तर को कम रखना । इन सिद्धांतों का पालन करते हुए जिस इस्पात का विकास हुआ वह अधिक विकिरण का सामना कर सकता है और इसमें कुछ ऐसे पदार्थ जो इसको भंगुर बना सकते हैं उनकी मात्रा कम कर दी गई है । इन सब पदार्थों के विकास में निर्वात प्रेरण गलन (वैक्यूम इंडक्शन मेल्टिंग) के बाद निर्वात शोधन (वैक्यूम रिफाइनिंग) का प्रयोग किया गया है और इन सब तकनीकों का प्रयोग करने से एक ऐसे सम्मिश्र की उत्पति होती है जिसकी गुणवत्ता बहुत अच्छी है । Cr-W Ta-C की मात्रा उपयुक्त की गई है ताकि इसकी भार वहन क्षमता उत्तम रहे और भंगुरपन न आए । इस इस्पात के निर्माण के पश्चात इसका नोरमलाइज़िंग और टेंपरिंग किया जाता है । संलयन ऊर्जा के उत्पत्ति में प्रयोग किये जाने वाले पदार्थों में दूसरा उदाहरण लीथियम टाइटेनेट के बारे में कहा जा सकता है जिसका प्रयोग टेस्ट ब्लैंकेट मॉडल में प्रयोग किये जाने वाले पदार्थों में एक उत्तम पदार्थ है क्योंकि इसकी तापीय स्थिरता उत्तम है और ट्रिशियम बनाने का काम ये कम तापमान पर कर सकता है इसकी ताप चालकता

बहुत अच्छी है। दूसरे पदार्थ जैसे लीथियम जिरकनेट एवं लीथियम सिलिकेट की तुलना में इस पदार्थ का प्रयोग बेहतर है और छोटे गोल आकार के पदार्थ का मूल्यांकन किया जा रहा है ताकि इसका प्रयोग टी.बी.एम. में ट्रिशियम उत्पादन के लिए किया जा सके । इसे बनाने का लिए दो तरह के ऑक्साइड्स का प्रयोग किया जाता है । दोनों ऑक्साइड्स को मिश्रित करने के बाद एक आकार दिया जाता है । इसमें ऊर्जा उत्पादन के बाद भी करीब ४५% Li आइसोटोप बच जाता है । जिसको निकाल कर फिर से प्रयोग किया जा सके, इसके लिए ऐसी विधि का विकास किया जा रहा है ताकि लीथियम को लीथियम टाइटेनेट से निकाला जा सके ।

इसके अलावा और जिन पदार्थों का विकास संलयन कार्यक्रम के लिए किया गया है वह हैं-

१. प्लाज़्मा उन्मुख निम्न परमाणु क्रमांक (Z) एवं उच्च परमाणु क्रमांक पदार्थ ।

२. हीटसिंक हेतु का पर सम्मिश्र।

३. संरचनात्मक– आस्टेनिटिक स्टील, निम्न एक्टिवेशन फेरिटिक मार्टेंसिटिक स्टील एवं ओ.डी.एस. स्टील ।

४. नियोबियम–टाइटेनियम एवं नियोबियम–टिन अतिचालक पदार्थों का विकास ।

५. लेड-बिस्मिथ शीतलक ।

सिरेमिक के क्षेत्र में कुछ उदाहरण

बोरोन कारबाईड, टाईटेनियम बोराईड, रेयर अर्थ बोराईड और जिरकोनियम डाई बोराइड, इनका प्रयोग इलेक्ट्रानिकी में एवं रिएक्टर के विभिन्न भागों में रिएक्टर को नियंत्रित करने में किया जाता है इसके अलावा इनका प्रयोग गोलीरोधक (बुलेट प्रूफ) जैकेट को बनाने के लिए भी किया जाता है । भा. प. अ. केंद्र द्वारा विकसित गोलीरोधक जैकेट वजन में हल्का और गोलियों को रोकने की क्षमता में उत्तम है।

अंतिम उदाहरण धातु-कांच का है जो सम्मिश्र को बहुत तेजी से ठंडा करके बनाया जा सकता है । ठंडा करने की दर एक लाख डिग्री प्रति सेकेंड होनी चाहिए । ऐसी स्थिति में धातु को ग्लास (कांच) के रूप में बनाया जा सकता है । इस कांच के बहुत महत्वपूर्ण गुण होते हैं जिसके कारण इनका प्रयोग कई क्षेत्रों में किया जा सकता है । इन कांचके उपयोग दैनिक जीवन में काम आने वाले कुछ उपकरण जैसे सेलफ़ोन के केसिंग एवं रक्षा विभाग के लिए कई संयंत्रो के निर्माण में किया जा सकता है ।

नाभिकीय ऊर्जा से बिजली उत्पादन के अतिरिक्त नाभिकीय क्षेत्र में अनेकानेक पदार्थ प्रौद्योगिकियों के विकास के साथ आज भारत विश्व के अग्रणी देशों में एक है । ऐसे ही कुछ पदार्थ हैं–

१. सिलिकॉन कार्बाइड, बेरिलियम, कोबाल्ट, न्यूट्रान सेंसर, लेड-लिथियम सीलेंट, धात्विक कांच, उच्चताप अतिसुचालक नमूना मोटर, विद्युतधारा प्रतिबंधक यंत्र ।

२. रेडियो समस्थानिक के लिए कोबाल्ट पाउडर से कोबाल्ट स्लग एवं पैलेट

३. जीऍमआर आधारित न्यूट्रान सेंसर का विकास

४. हाइड्रोजन शमन के लिये उत्प्रेरक कार्डों का निर्माण

५. चिकित्सा में प्रयुक्त भाभाट्रान के घटकों पर Ni की इलेक्ट्रो प्लेटिंग का विकास >100 इकाइयां

६. विसरण आधारित जोड़ बनाने के लिये अंतर परतों का विकास

७. ग्रेफाइट शीतलक ट्यूब

८. रिफ्रैक्टरी धातु एवं सम्मिश्र

९. बेरिलियम

१०. लेड-बिस्मिथ शीतलक

११.ऊष्मा उपचारित जर्कोनियम एलाय का विकास

१२. ट्राइसोलेपित–सुरक्षा में वृद्धि, विखंडित पदार्थ लेपित ईंधन कणों के अंदर, ज्यादा बर्न-अप

१३. कांच–सेरिमिक, कांच-धातुजोड़-विकास एवं निर्माण

१४. सेंसर एवं एक्चुएटर के लिए पीजो-इलेक्ट्रिक एवं रिलैक्सर सिरेमिक पदार्थों का निर्माण, ठोस आक्साइड ईंधन सेल घटकों के लिये पदार्थों का विकास

१५.वैनेडियम के विभिन्न एलाय का विकास

१६.नियोबियम–टाइटेनियम एवं नियोबियम–टिन अतिचालक पदार्थों का विकास

१७. पदार्थों पर अध्ययन के लिए कई सुविधाओं का विकास इन सभी उपलब्धियों को प्राप्त करने में भा.प.अ. केंद्र एवं परमाणु ऊर्जा विभाग की अन्य इकाइयों के बहुत सारे वैज्ञानिकों ने अपना योगदान दिया है।

आभार

इस लेख को तैयार करने में डा.कुलवंत सिंह एवं श्रीमती शर्मिला डे द्वारा सहयोग दिया गया जिसके लिए लेखक उनके आभारी हैं।

संबधित लेखक एवं ई-मेल: डॉ. जी. के. डे ,

(gkdey@barc.gov.in)

IAEA Technical Meeting on Underground Research Facility Network

Shri Kailash Agarwal, Former Director, Nuclear Recycle Group, BARC, delivering inaugural address

The Global Centre for Nuclear Energy Partnership (GCNEP) and the Nuclear Recycle Group of Bhabha Atomic Research Centre jointly hosted the last edition of IAEA Technical Meeting on Underground Research Facility Network held during May 21-25, 2018, at GCNEP in Bahadurgarh in Haryana.

The theme meeting titled 'Global Progress in Geological Disposal Solutions for Radioactive Waste' is a part of regular technical consultations on Deep Geological Repository (DGR) and Underground Research Facilities (URF) worldwide, under the leadership of the IAEA.

A total of 13 foreign delegates participated in the meeting coming from Switzerland, South Africa, China, Republic of Korea, Lithuania, Germany, Czech Republic, France, Canada, Ukraine, Japan and India. Indian participation included observers and experts from BARC Mumbai, BARC Tarapur, IGCAR Kalpakkam and GCNEP Haryana.

Dr. R.K. Bajpai, Head, Repository Engineering Section of Nuclear Recycle Group, and Mr. Stefan Mayer, Group Leader, Waste Technology Section, IAEA, acted as conveners of the technical meeting from India and IAEA, Vienna, respectively.

The meeting covered the latest global technological developments in geological disposal projects for High Level Long Lived radioactive waste. The future strategic orientation of the programme of work with a view to identify specific activities and topics to be addressed by the URF Network in 2019 and beyond was also presented in the 5-day meeting.

An exhibition comprising models, posters and samples depicting main components of Indian radioactive waste management and disposal programme was organised as part of the meeting. The inaugural function was followed by detailed presentations on Deep Geological Repository (DGR) & Underground Research Facilities (URF) projects in member states, IAEA presentations, discussions of future program and new documents.

The IAEA Scientific Secretary gave a detailed presentation on the status of two documents being prepared by IAEA URF Network namely Roadmap to Deep Geological Repository (DGR) and Compendium of URF. The member states proposed that IAEA may initiate a programme

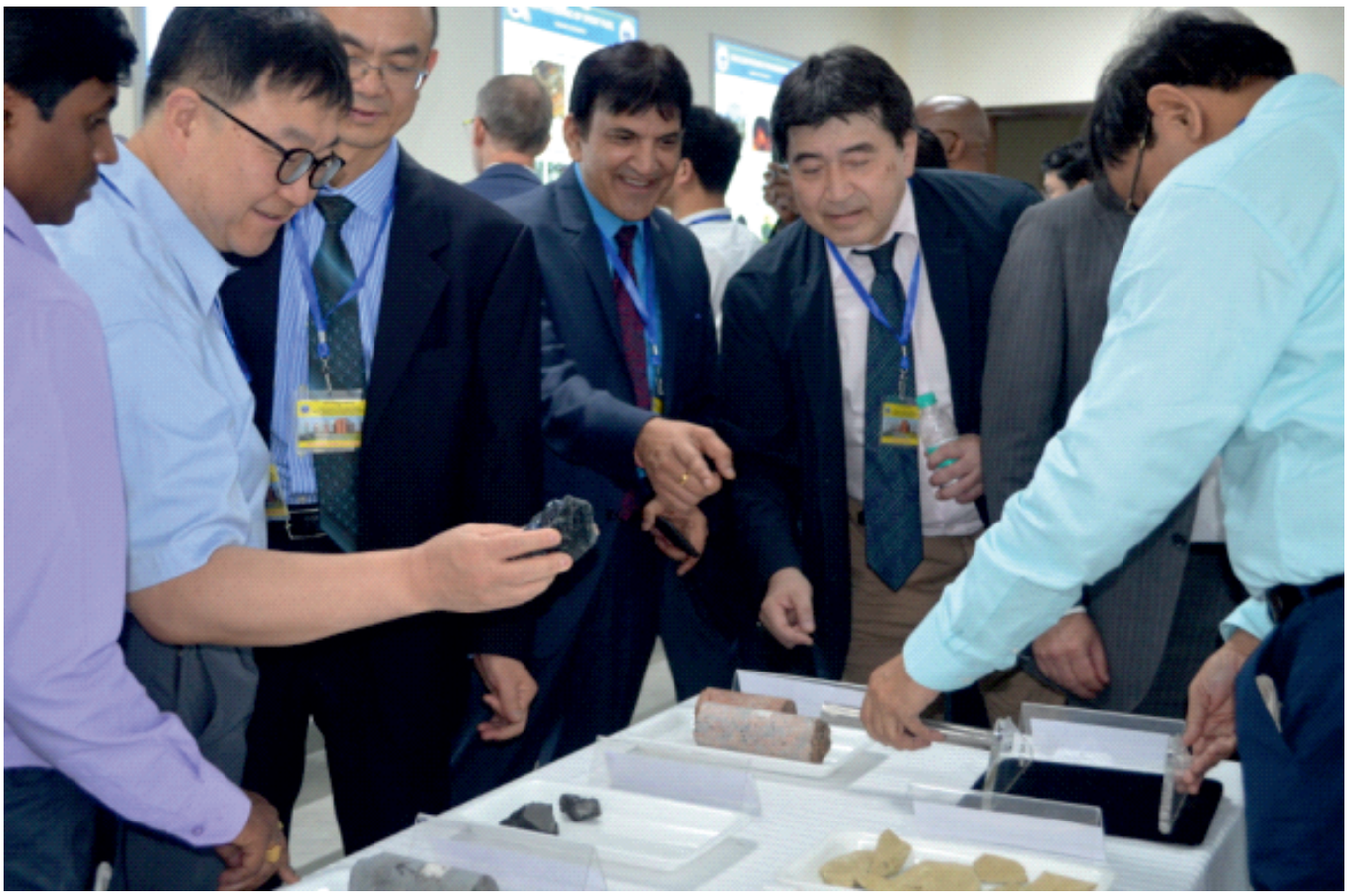

International delegates visiting the Radioactive Waste Management and Disposal exhibition during the 5-day meeting

to develop a new document dealing with site selection criteria on DGR and URF.

The IAEA also explored the possibility of holding related training programmes/fellowships in the member states. Participation in URF experiments in the member states through joint funding and data sharing emerged as one of the possible mechanism for providing access to methodology and technology-under-development.

The member states also proposed that the agency may initiate few CRP's to deal with Total System Performance Assessment of DGR, Long term safety assessment methodology for DGR, Corrosion studies, radionuclide migrations in DGR. IAEA assured to explore the possibility in this regard. The next meeting of URF Network will take place in China's Beishan URF in September 2019.

Central Complex BARC

Edited & Published by:
Scientific Information Resource Division
Bhabha Atomic Research Centre, Trombay, Mumbai 400 085, India
BARC Newsletter is also available at URL:http://www.barc.gov.in